P17 induces chemotaxis and differentiation of monocytes via MRGPRX2-mediated mast cell–line activation

Karthi Duraisamy, Kailash Singh, Mukesh Kumar, Benjamin Lefranc, Elsa Bonnafé, Michel Treilhou, Jérôme Leprince, Billy K.C. Chow

▶ **To cite this version:**

Karthi Duraisamy, Kailash Singh, Mukesh Kumar, Benjamin Lefranc, Elsa Bonnafé, et al.. P17 induces chemotaxis and differentiation of monocytes via MRGPRX2-mediated mast cell–line activation. Journal of Allergy and Clinical Immunology, 2022, 149 (1), pp.275-291. 10.1016/j.jaci.2021.04.040 . hal-04144398

HAL Id: hal-04144398
https://hal.science/hal-04144398v1

Submitted on 24 May 2024

HAL is a multi-disciplinary open access archive for the deposit and dissemination of scientific research documents, whether they are published or not. The documents may come from teaching and research institutions in France or abroad, or from public or private research centers.

L'archive ouverte pluridisciplinaire **HAL**, est destinée au dépôt et à la diffusion de documents scientifiques de niveau recherche, publiés ou non, émanant des établissements d'enseignement et de recherche français ou étrangers, des laboratoires publics ou privés.

Distributed under a Creative Commons Attribution - NonCommercial - NoDerivatives 4.0 International License

P17 induces chemotaxis and differentiation of monocytes via MRGPRX2-mediated mast cell–line activation

Karthi Duraisamy, PhD,[a] Kailash Singh, PhD,[a] Mukesh Kumar, MS (Pharm),[a] Benjamin Lefranc, MS,[b] Elsa Bonnafé, PhD,[c] Michel Treilhou, PhD,[c] Jérôme Leprince, PhD,[b] and Billy K. C. Chow, PhD[a] *Hong Kong, China; and Rouen and Albi, France*

GRAPHICAL ABSTRACT

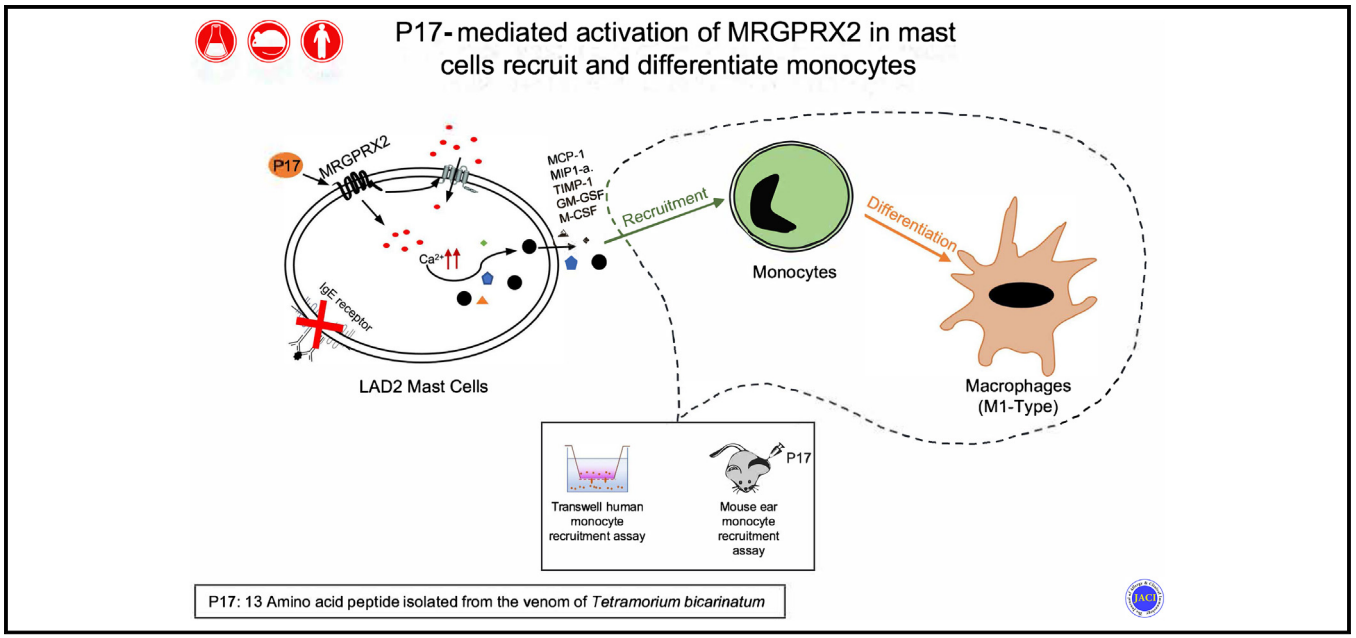

Background: P17, a peptide isolated from *Tetramorium bicarinatum* ant venom, is known to induce an alternative phenotype of human monocyte–derived macrophages via activation of an unknown G protein–coupled receptor (GPCR).
Objective: We sought to investigate the mechanism of action and the immunomodulatory effects of P17 mediated through MRGPRX2 (Mas-related G protein–coupled receptor X2).
Methods: To identify the GPCR for P17, we screened 314 GPCRs. Upon identification of MRGPRX2, a battery of *in silico*, *in vitro*, *ex vivo*, and *in vivo* assays along with the receptor mutation studies were performed. In particular, to investigate the immunomodulatory actions, we used β-hexosaminidase release assay, cytokine releases, quantification of mRNA expression, cell migration and differentiation assays, immunohistochemical labeling, hematoxylin and eosin, and immunofluorescence staining.
Results: P17 activated MRGPRX2 in a dose-dependent manner in β-arrestin recruitment assay. In LAD2 cells, P17 induced calcium and β-hexosaminidase release. Quercetin- and short hairpin RNA–mediated knockdown of MRGPRX2 reduced P17-evoked β-hexosaminidase release. *In silico* and *in vitro* mutagenesis studies showed that residue Lys^{8} of P17 formed a cation-π interaction with the Phe^{172} of MRGPRX2 and [Ala^{8}] P17 lost its activity partially. P17 activated LAD2 cells to recruit THP-1 and human monocytes in Transwell migration assay,

From [a]the School of Biological Sciences, The University of Hong Kong, Hong Kong; [b]INSERM U1239, PRIMACEN, IRIB, Normandy University, Rouen; and [c]EA7417 BTSB, Université Fédérale Toulouse Midi-Pyrénées, INU Champollion, Albi.

This work was supported by the HK government Research Grants Council (RGC) grant (nos. GRF 1711320 and 17111421), National Natural Science Foundation of China/RGC, and University of Hong Kong seed fund for basic research (grant no. 201910159222 to B.K.C.C.); Institut National de la Santé et de la Recherche Médicale (Inserm), the Normandy University (Rouen), the Region Normandy, the European Union (PHEDERCPG and 3R projects), and Europe gets involved in Normandy with European Regional Development Fund to J.L.

Disclosure of potential conflict of interest: The authors declare that they have no relevant conflicts of interest.

Received for publication August 15, 2020; revised March 29, 2021; accepted for publication April 23, 2021.

Available online June 7, 2021.

Corresponding author: Billy K. C. Chow, PhD, School of Biological Sciences, HKU, Hong Kong. E-mail: bkcc@hku.hk. Or: Jérôme Leprince, PhD, INSERM U1239, France. E-mail: jerome.leprince@univ-rouen.fr.

The CrossMark symbol notifies online readers when updates have been made to the article such as errata or minor corrections

0091-6749

© 2021 The Authors. Published by Elsevier Inc. on behalf of the American Academy of Allergy, Asthma & Immunology. This is an open access article under the CC BY-NC-ND license (http://creativecommons.org/licenses/by-nc-nd/4.0/).

https://doi.org/10.1016/j.jaci.2021.04.040

whereas MRGPRX2-impaired LAD2 cells cannot. In addition, P17-treated LAD2 cells stimulated differentiation of THP-1 and human monocytes, as indicated by the enhanced expression of macrophage markers cluster of differentiation 11b and TNF-α by quantitative RT-PCR. Immunohistochemical and immunofluorescent staining suggested monocyte recruitment in mice ears injected with P17.
Conclusions: Our data provide novel structural information regarding the interaction of P17 with MRGPRX2 and intracellular pathways for its immunomodulatory action. (J Allergy Clin Immunol 2022;149:275-91.)

Key words: *Mast cell activation, innate immunity, immune modulation, MRGPRX2, mast cells, monocytes, human-monocyte–derived macrophages (h-MDMs), monocyte recruitment, chemotaxis, cytokine release*

Abbreviations used

aa:	Amino acid
CD11a:	Cluster of differentiation 11a
CD11b:	Cluster of differentiation 11b
CD11c:	Cluster of differentiation 11c
CD14:	Cluster of differentiation 14
CST-14:	Cortistatin-14
DRG:	Dorsal root ganglia
ECL:	Extracellular loop
GPCR:	G protein–coupled receptor
HDP:	Host defense peptide
h-MDM:	Human-monocyte–derived macrophage
ICAM-1:	Intercellular adhesion molecule 1
MC:	Mast cell
MCP1:	Monocyte chemoattractant protein 1
MD:	Molecular dynamics
MIP-1α:	Macrophage inflammatory protein 1 α
MRGPRX2:	Mas-related G protein–coupled receptor X2
shRNA:	Short-hairpin RNA
TM:	Transmembrane

Venomous animals have developed a vast array of venom peptides for protection and predation. These peptides are invaluable resources to mankind because they are already directed to various pharmacological targets that are potentially related to pathological conditions.[1] Currently, there are at least 10 Food and Drug Administration–approved drugs available in the market based on animal venom peptides.[2] These peptides, termed host defense peptide (HDP), are an evolutionarily essential component of the innate immune system of most multicellular organisms.[3] They have gained importance in recent years due to their broad spectrum of antimicrobial activities and their emerging role in innate and adaptive immune responses.[4] There are 2 families of naturally occurring HDPs found in humans—defensins and cathelicidins. Defensins have been shown to play a role as immune modulators by inducing production of proinflammatory cytokines and act as chemokines for various immune cells and enhance the phagocytic ability of macrophages.[5] Cathelicidins such as peptide LL-37 act as chemoattractant for neutrophils, monocytes, and T cells by interacting with the formyl peptide receptor–like 1, a G protein–coupled receptor (GPCR).[6,7] Moreover, they are involved in wound healing by acting as an angiogenic factor.[8,9] Some individual HDPs could use more than 1 GPCR to facilitate their functions in different cells. For instance, human β-defensin 3 is chemotactic to dendritic cells via chemokine receptor 6 and monocytes via an unknown GPCR.[10] The multidimensional properties of these HDPs hold promising potentials as prophylactic and antimicrobial agents via direct activation and recruitment of concomitant immune cells.

P17 is a short HDP characterized from the ant *Tetramorium bicarinatum* venom[11] recently shown to be involved in host defense by activating macrophages.[12] Therefore, it is hypothesized that P17 can be exploited as a therapeutic peptide for the treatment of immune-related diseases. In our previous study, we have shown that P17 induces an alternative phenotype of human-monocyte–derived macrophages (h-MDMs) by activating an unknown *pertussis* toxin–sensitive GPCR via calcium mobilization, which in turn enhances the antifungal activity of h-MDMs.[12] GPCRs are the largest family of membrane proteins in human genome as it encodes for approximately 800 of these 7 transmembrane (TM) receptors, which are about 13% of all membrane proteins.[13-16] GPCRs serve as increasingly attractive drug targets due to their important roles in various physiological processes and relevance in diseases such as inflammatory disorders, metabolic imbalances, cardiac disorders, and cancer as well.[15,17] GPCRs can be classified into 6 classes sharing similar structural properties with the core 7 TM domains, variable extracellular N-terminal and intracellular C-terminal extensions, and 3 extracellular loops (ECLs) and 3 intracellular loops. On ligand binding, GPCRs undergo conformational changes, which result in various intracellular modifications via G protein–dependent (eg, cyclic adenosine 3',5'-cyclic monophosphate and phospholipase C) and G protein–independent (eg, β-arrestin) pathways.[18-23] To date, structures of about 50 GPCRs have been resolved. The recent advances in both structural and molecular studies have enabled new computational methods to discover novel ligand-binding sites that modulate GPCR functions.[24] As mentioned above, the identity of GPCRs corresponding to P17 is unknown. Therefore, in this study, we have identified Mas-related G protein–coupled receptor-X2 (MRGPRX2) as a first specific receptor for peptide P17, because there is a possibility that more than 1 GPCR may recognize P17.

Rhinitis, asthma, food allergy, and eczema are common allergic diseases that affect more than 50 million people in the United States, with an annual cost of $18 billion. The adverse effects of allergic diseases highlight the importance of novel and alternative therapeutic methods in tackling these chronic conditions. In particular, the critical role of mast cells (MCs) in the manifestation of systemic allergic reaction is crucial.[25] MC release constitutes a major role in anaphylaxis, and in the case of the minor acute MC degranulation, it may result in the initiation of systematic and complex inflammatory pathways, which are often used for host defense against various venoms and parasites.[26] MRGPRX2 is a membrane GPCR, almost exclusively expressed in immune MCs, and is responsible for MC-mediated clinically relevant hypersensitive reactions in the absence of severe allergic reactions.[27] For instance, LL-37 is a known agonist of MRGPRX2, which is highly upregulated in rosacea.[28] MCs are the major source of LL-37 in the murine model of rosacea.[26,29] In fact, many allergens that activate MRGPRX2 have not been validated for specificity or potency,[30,31] and these compounds have to be investigated in detail. In this study, we show that via

MC activation, P17 induces recruitment and differentiation of monocytes into macrophages. Taken together, our data thus provide structural information of P17 interacting with MRGPRX2 and its intracellular pathways for an immunomodulatory action.

METHODS

Animals

C57BL/6N adult male mice, about 6 to 8 weeks old, were obtained from the Laboratory Animal Unit of the University of Hong Kong (AAALAC International accredited). This study was conducted in strict accordance with the recommendations stated in the Guide for the Care and Use of Laboratory Animals of the National Institutes of Health. Protocols of the study were approved by the Committee on the Use of Live Animals in Teaching and Research (CULATR 4849-19) of the University of Hong Kong. All animal procedures were performed under ketamine/xylazine anesthesia.

PRESTO-Tango GPCR β-arrestin recruitment assay

β-Arrestin recruitment assay was carried out as previously described.[32] For antagonistic study, compounds/peptides were added 1 hour before adding the agonists. On day 5, medium and drug solutions were removed from the wells (by aspiration) and 30 μL luciferase substrate solution was added to each well. After incubation for 10 minutes at room temperature, luminescence was counted in PerkinElmer Victor X4.

Intracellular calcium assay

Chinese hamster ovary-K1 cells were seeded at a density of 2.0×10^5 per well onto 6-well plates (Nunc) using minimum essential medium 24 hours before transfection with lipofectamine 2000 Transfection Reagent (Invitrogen, Waltham, Mass). Twenty-four hours after transfection, the cells were lifted using Gibco Versene Solution, and 5×10^4 cells were transferred to 35-mm glass-bottom Petri dishes (MatTek Corporation, Ashland, Mass) overnight for confocal microscopy and 2×10^4 cells were plated in 96-well plates for dose-response experiments. Fluo4-NW assay kit (Thermo Fisher Scientific, Waltham, Mass) was used for detecting the intracellular calcium as specified by the manufacturer.

Real-time quantitative RT-PCR

First-strand cDNAs were obtained (Transcriptor First Strand cDNA Synthesis Kit, Roche Diagnostics GmbH, Mannheim, Germany), followed by quantitative PCR (7300 Real-Time PCR System, Applied Biosystems, Foster City, Calif). The expression of transcripts was examined using ChamQ SYBR Color qRT-PCR Master Mix as specified by the manufacturer. $2^{-\Delta\Delta Ct}$ method[33] was used for data analysis with the internal control, *gapdh*.

The β-hexosaminidase release assay

The β-hexosaminidase release assay was carried out as we previously described.[32] Either P17 or other agonists at the indicated concentrations diluted in modified Tyrode's solution were introduced into each well and incubated for 30 minutes. For antagonistic study, compounds/peptides were added 30 minutes before adding the agonists. Compound 48/80 was used as a positive control.[34]

Lentivirus production and MRGPRX2 silencing in LAD2 cells

MRGPRX2-targeted Mission short-hairpin RNA (shRNA) lentiviral plasmids were purchased from Sigma-Aldrich, St Louis, Mo. We used 2 shRNAs for lentiviral production, and a nontarget shRNA vector was used as a control. SHC016**,** TRCN0000357642, and TRCN0000009176 were used to produce lentivirus, according to the manufacturer's instructions. Cell transduction was conducted by mixing 2 mL viral supernatant with 3 mL LAD2 (5×10^6) cells. Eight hours after infection, medium was changed to virus-free complete medium, and antibiotic (puromycin, 2 μg/mL; Sigma-Aldrich) selection was initiated 16 hours later. Cells were analyzed for MRGPRX2 knockdown by real-time quantitative RT-PCR (qRT-PCR).[35]

Quantification of Evans blue

Quantification of Evans blue was carried out as previously described[32] with slight modification. Young adult mice (C57BL/6N aged 6-8 weeks old) were intravenously injected with 50 μL (irrespective of the body weight) of 12.5% Evans blue in saline. Five minutes later, 5 μL of 20 μg/mL agonists was injected into one paw, and saline was injected into the other paw as a negative control. For antagonist study, the antagonist was introduced 10 minutes before agonists. Fifteen minutes later, the paw thicknesses were measured again and documented. Mice were euthanized and paw tissues were collected, dried at 50°C, and weighed separately. Evans blue dye is extracted by adding 500 μL of a mixture of acetone-saline (7:3) to each tissue sample and incubating at 37°C for 12 hours.

Identification of P17 binding site on MRGPRX2 receptor

MRGPRX2 receptor belongs to opioid receptor family. All class A GPCRs are generally known to have their active site at the TM domain, largely adapted as a binding site for small compound agonists, such as P17, which is a 13-amino acid (aa) long peptide. For molecular dynamics (MD) simulation, the homology model of receptor and peptide was merged and corrected for abnormalities by protein preparation wizard and was later embedded in hydrolyzed 8 × 8 nm 1-palmitoyl-2-oleoyl-sn-glycero-3-phosphocholine lipid bilayer structure. The system was submitted to steepest-descent energy minimization up to a tolerance of 1000 KJ/mol/nm and was evaluated by protein-ligand root root-mean-square deviation (RMSD) analysis for the 200 ns of simulation time. We have performed a preliminary study of single unbiased MD simulation of 200 ns in which the P17 peptide started the interaction process with the MRGPRX2 model. We performed site-directed mutagenesis on Tango-MRGPRX2 for the above-mentioned aa using the Q5 Site-Directed Mutagenesis Kit (New England BioLabs, Ipswich, Mass). The mutant Tango-MRGPRX2 receptors were used for PRESTO-Tango GPCR β-arrestin recruitment assay.

Pharmacophore region and alanine scanning of peptide P17

In an attempt to locate the pharmacophore region of P17, we have synthesized 8 truncated P17 analogues—$P17_{(3\text{-}13)}$, $P17_{(5\text{-}13)}$, $P17_{(7\text{-}13)}$, $P17_{(9\text{-}13)}$, $P17_{(1\text{-}5)}$, $P17_{(1\text{-}7)}$, $P17_{(1\text{-}9)}$, and $P17_{(1\text{-}11)}$—and 12 peptides by replacing each aa of peptide P17 with alanine.[36] All these compounds were functionally tested for standard degranulation β-hexosaminidase assays in LAD2 cells. P17, downsized and alanine-substituted analogues were synthesized by Fmoc solid-phase methodology on a Liberty microwave-assisted automated peptide synthesizer (CEM, Saclay, France) using the standard manufacturer's procedures at 0.1 mmol scale as previously described.[37] All Fmoc-amino acids (0.5 mmol, 5 eq.) were coupled on preloaded Fmoc-Leu-, Fmoc-Ile-, Fmoc-Glu(O*t*Bu)-, or Fmoc-Ala-Wang resin by *in situ* activation with HBTU (0.5 mmol, 5 eq.) and DIEA (1 mmol, 10 eq.), and Fmoc removal was performed with a 20% piperidine solution in DMF. After completion of the chain assembly, peptides were deprotected and cleaved from the resin by adding 10 mL of the mixture TFA/TIS/H_2O (9.5:0.25:0.25) for 180 minutes at room temperature. After filtration, crude peptides were washed thrice by precipitation in TBME followed by centrifugation (4500 rpm, 15 minutes). The synthetic peptides were purified by reversed-phase HPLC on a 21.2 × 250 mm Jupiter C_{18} (5 μm, 300 Å) column (Phenomenex, Le Pecq, France) using a linear gradient (10%-50% or 10%-40% over 45 minutes) of acetonitrile/TFA (99.9:0.1) at a flow rate of 10 mL/min. The purified peptides were then characterized by MALDI-TOF mass spectrometry on an UltrafleXtreme (Bruker, Strasbourg, France) in the reflector mode using α-cyano-4-hydroxycinnamic acid as a matrix. Analytical reversed-phase-HPLC, performed on a 4.6 × 250 mm Jupiter

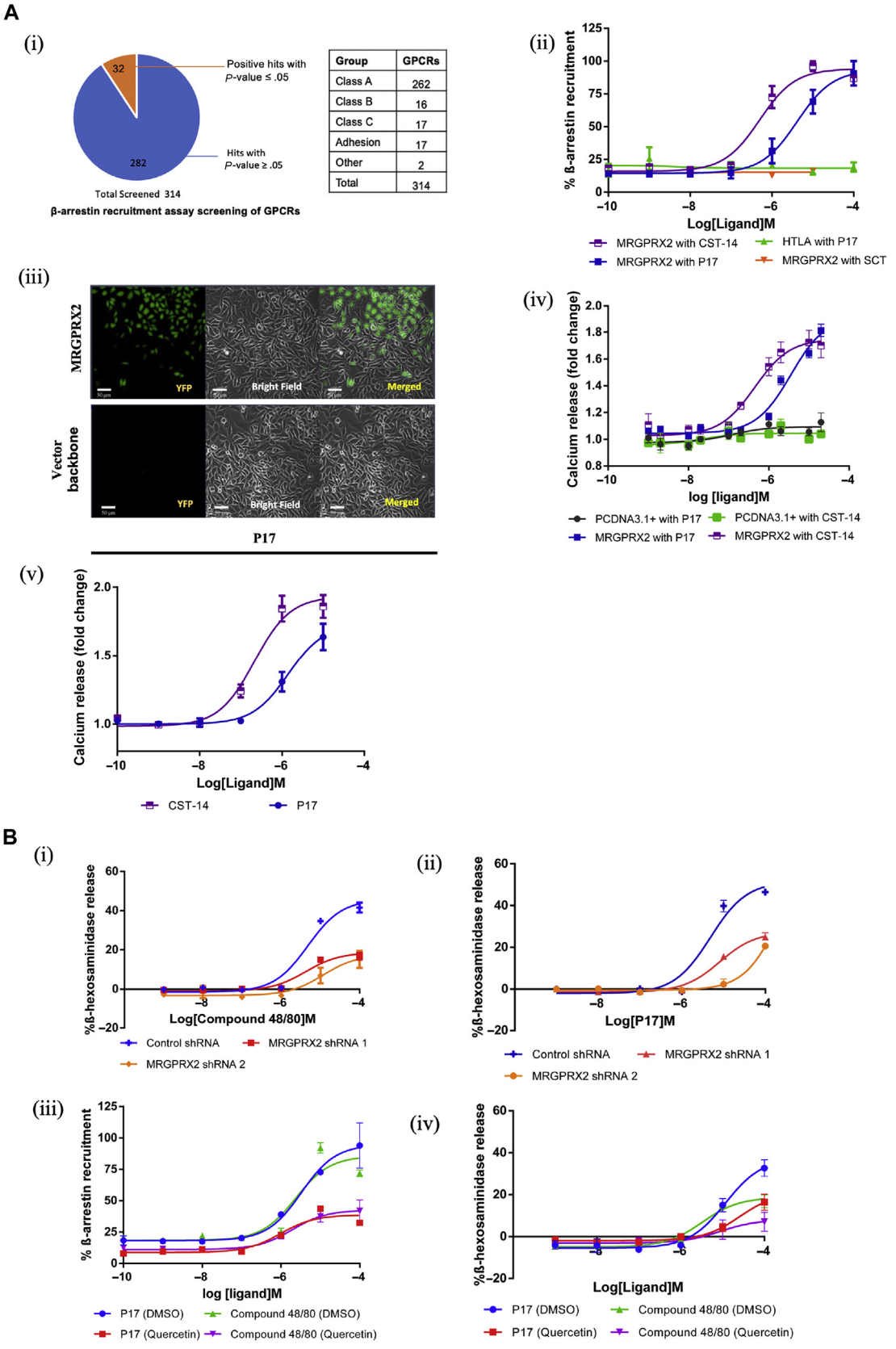

FIG 1. Identification of MRGPRX2 as the receptor for P17 and using 3-D homology modeling to show certain aas are involved in peptide-receptor interactions. **A,** (**i**) Chart showing the total number of GPCRs screened ($P \leq .05$). (**ii**) Dose-dependent Tango-MRGPRX2 β-arrestin recruitment assay of P17 (N = 3-5) ($P \leq .0001$). (**iii**) Representative live cell confocal images showing P17-mediated Ca^{2+} release. P17 (2.5 μM)-treated

C_{18} (5 μm, 300 Å) column, indicated that the purity of the peptides was more than 99.%.

Human monocyte isolation

Human monocytes were isolated essentially according to the previously published protocol.[38] Briefly, whole blood was collected from healthy volunteer donors in EDTA tubes (4 mL) and added to tubes containing Ficoll-Paque Plus (4 mL) (Cytiva). Tubes were centrifuged to collect the buffy coat, which was then washed 3 times with 40 mL serum-free RPMI media by centrifugation (400*g*, 10 minutes). Cells were resuspended in serum containing RPMI 1640 media and plated in 100-mm culture dish for 4 hours. The adhered monocytes at the culture disk were subsequently verified by flow cytometry analysis with cluster of differentiation 11b (CD11b) and cluster of differentiation 14 (CD14) markers.

In vitro cell invasion and migration assays

In vitro cell invasion assays were performed in 12-mm diameter and 3-μm-pore polycarbonate filter transwell plates (Corning Transwell polycarbonate membrane cell culture inserts). THP-1 cells (2×10^5 cells in 300 μL RPMI-1640 medium) were seeded on the upper chamber, and the lower well filled with wild-type and MRGPRX2 knockdown LAD2 cell supernatants as chemoattractant (700 μL, serum-free StemPro-34) that was previously exposed to water, P17, and compound 48/80. Water was used as a negative control. After incubation for 16 to 18 hours at 37°C in the presence of 5% CO_2, THP-1 cells were fixed for 15 minutes in methanol and stained for 5 to 10 minutes with 0.1% crystal violet. Cells that had migrated or invaded to the bottom surface of the filter were counted.[39]

Cell culture and differentiation assay

THP-1 or human primary monocytes were cultured at an initial density of 5×10^5 cells/mL (1 mL) and treated with serum-free Stempro-34 supernatants (1 mL) collected from LAD2 cells treated with P17, compound 48/80, or water for 24 to 48 hours in a 6-well plate. THP-1 cells were then collected for real-time qRT-PCR and/or flow cytometry assays.

Immunohistochemistry, hematoxylin and eosin, and immunofluorescence staining

Animals were sacrificed and ears were isolated from mice and fixed in 10% formaldehyde, dehydrated with graded ethanol, embedded in paraffin, and sectioned (10 μm). Immunostaining, hematoxylin and eosin staining, and immunofluorescence were carried out as previously described.[40] Rabbit anti-CD11b antibody (1:500 dilution; Abcam, Cambridge, UK) was used as the primary antibody. Alexa Fluor 488 donkey antirabbit IgG (1:500 dilutions; Invitrogen) was used for immunofluorescence as the secondary antibody. For double staining, rabbit anti-CD11b (1:500 dilution; Abcam) and Rat anti-F4/80 [CI:A3-1] (1:200 dilution, Abcam) were used as primary antibodies, and Alexa Fluor 488 donkey antirabbit IgG (1:500 dilutions; Invitrogen) and Alexa Fluor 594 Goat Anti-Rat IgG (1:500 dilution; Abcam) were used as secondary antibodies. Statistical comparisons were made between the number of CD11b-positive cells in ear areas in control and treated groups using Student *t* test, with significance set at *P* value less than or equal to .05.

Quantification and statistical analysis

All data are shown as means ± SEM unless specified. The graphs between groups were plotted using Prism 8.0 software (GraphPad Software Inc, San Diego, Calif). The data were analyzed using Student *t* tests and ANOVA (2-way ANOVA) followed by Tukey's multiple comparisons test throughout this study. A *P* value of less than or equal to .05 was considered to be significant.

Detailed methodology is available in this article's Methods section in the Online Repository at www.jacionline.org.

RESULTS

Identification of MRGPRX2 as a receptor for P17 and 3-dimensional homology modeling to determine specific aa residues involved in peptide-receptor interactions

To identify a specific receptor for P17, a dose of 100 nM was used to screen 314 Tango-GPCRs (Fig 1, *A*i) (Addgene), and initially 32 putative hits with *P* value less than or equal to .05 were obtained, of which 31 belonged to class A GPCR and 1 was a class B GPCR (PTH1R) (see Fig E1 in this article's Online Repository at www.jacionline.org). Among these hits, human Tango-MRGPRX2 was found to be dose-dependently activated by P17 with an EC_{50} value of 4.13 μM (95% CI, 1.85-9.18 μM), whereas cortistatin-14 (CST-14), a positive control, was able to activate MRGPRX2 with an EC_{50} of 0.49 μM (95% CI, 0.27-0.88 μM[31]) (Fig 1, *A*ii). Because MRGPRX2-mediated calcium release has been evidently reported before,[41,42] we have therefore evaluated the effect of P17 on Ca^{2+} mobilization in MRGPRX2-transfected CHO cells. Expression of MRGPRX2 mRNA in transfected cells was first verified by qRT-PCR (data not shown). Incubation of 2.5 μM P17 provoked calcium movements in the cytoplasm of MRGPRX2-transfected CHO cells (see video in this article's Online Repository at www.jacionline.org) (Fig 1, *A*iii) but not in control vector–transfected CHO cells. Application of graded concentrations of P17 and CST-14 induced dose-dependent increases in $[Ca^{2+}]_i$ with an EC_{50} of 3.5 μM (95% CI, 2.4-5.23 μM) and 0.44 μM (95% CI, 0.20-0.95 μM), respectively (Fig 1, *A*iv). Moreover, because MRGPRX2 is naturally expressed abundantly in a human MC model LAD2 cells,[43,44] we showed that both P17 and CST-14 induced $[Ca^{2+}]_i$ increases with EC_{50} of 1.42 μM (95% CI, 0.65-3.09 μM) and 0.21 μM (95% CI, 0.11-3.95 μM), respectively (Fig 1, *A*v).

To confirm that the effect of P17 on LAD2 cells is MRGPRX2-dependent, we have used lentiviral-mediated shRNA to knock down MRGPRX2 in LAD2 cells. MRGPRX2-impaired LAD2 cells by shRNA-mediated knockdown showed significant reduction in β-hexosaminidase release on both P17 and compound 48/80 treatments (Fig 1, *B*i and ii), indicating that P17 and compound 48/80 activated MCs via

MRGPRX2-PCDNA3.1+ transfected CHO cells and P17 (2.5 μM)-treated PCDNA3.1+ vector backbone transfected CHO cells (see videos in the Online Repository) (N = 3). (**iv**) Ca^{2+} response on graded concentration of P17 in MRGPRX2-transfected CHO cells (N = 3-4) ($P \leq .0001$). (**v**) Ca^{2+} mobilization in LAD2 cells on P17. **B,** Effect of P17 on MRGPRX2-impaired LAD2 cells. Percentage β-hexosaminidase release with (**i**) compound 48/80 and (**ii**) P17. Effect of quercetin on P17-evoked responses. (**iii**) Percentage β-arrestin recruitment in pretreated MRGPRX2-transfected HTLA cells with quercetin (100 μM). (**iv**) Percentage β-hexosaminidase release in pretreated LAD2 cells with quercetin (100 μM). All values are means ± SEM (N = 3 and n = 3). *DMSO*, Dimethyl sulfoxide; *ns*, not significant; *SCT*, Secretin; *YFP*, Yellow Fluorescent Protein. Compound 48/80 and CST-14 are positive controls. ****$P \leq .0001$; ***$P \leq .001$; **$P \leq .01$; * $P \leq .05$; and ns $P > .05$.

A

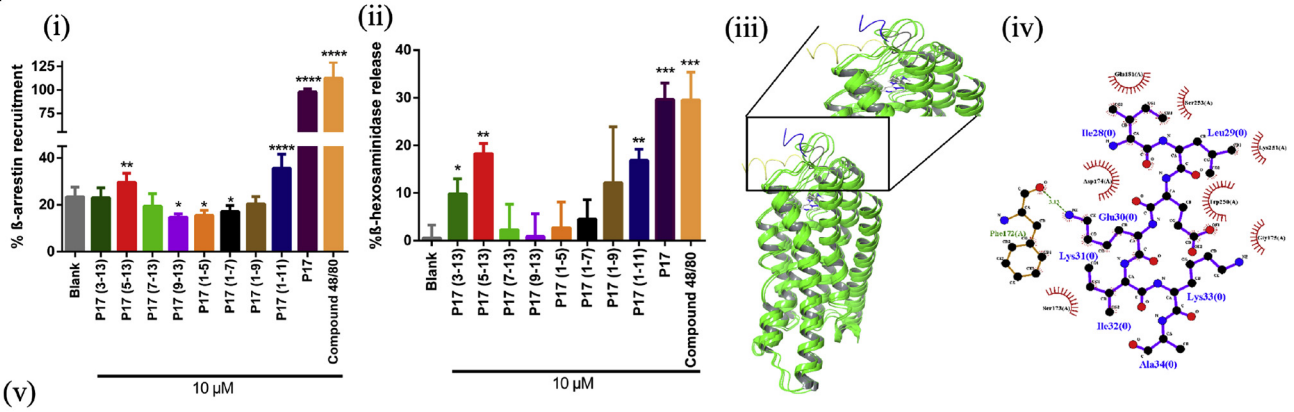

(v)

	Fragments	P17	Compound 48/80	CST-14	(Ala^1)P17	(Ala^2)P17	(Ala^3)P17	(Ala^4)P17	(Ala^5)P17	(Ala^6)P17	(Ala^7)P17	(Ala^8)P17	(Ala^9)P17	(Ala^{10})P17	(Ala^{12})P17	(Ala^{13})P17
TANGO ASSAY (% ß-arrestin recruitment)	EC_{50} (µM) (95% CI)	4.13 (1.85-9.18)	2.54 (0.78-7.94)	0.49 (0.27-0.88)	3.89 (2.29-6.63)	12.66 (7.33-21.91)	7.90 (5.01-12.46)	0.64 (0.17-2.30)	6.32 (3.52-11.36)	8.22 (5.03-13.45)	0.78 (0.28-2.22)	3.67 (0.21-65.36)	28.6 (17.67-46.48)	8.42 (3.13-22.63)	1.12 (0.10-22.63)	6.98 (4.08-11.93)
	Sign. Diff. (*P* value)		ns	****	**	*	ns	***	ns	ns	**	****	ns	*	**	ns
	E_{max}	100	76.24	96.08	105.76	71.27	93.19	107.12	85.62	79.58	90.71	34.5	96.66	60.63	54.29	102.15
%ß-Hexosaminidase release	EC_{50} (µM) (95% CI)	0.98 (0.61-1.57)	0.74 (0.33-1.64)	0.055 (0.038-0.078)		14.35 (9.28-22.20)		1.08 (0.79-1.48)			0.74 (0.43-1.288)	16.23 (12.48-21.11)		4.94 (3.10-7.88)	2.62 (1.57-4.37)	
	Sign. Diff. (*P* value)		*	****		****		***			***	****		****	ns	
	E_{max}	62.25	74.70	81.72		58.83		71.91			74.51	43.05		55.32	64.47	

B

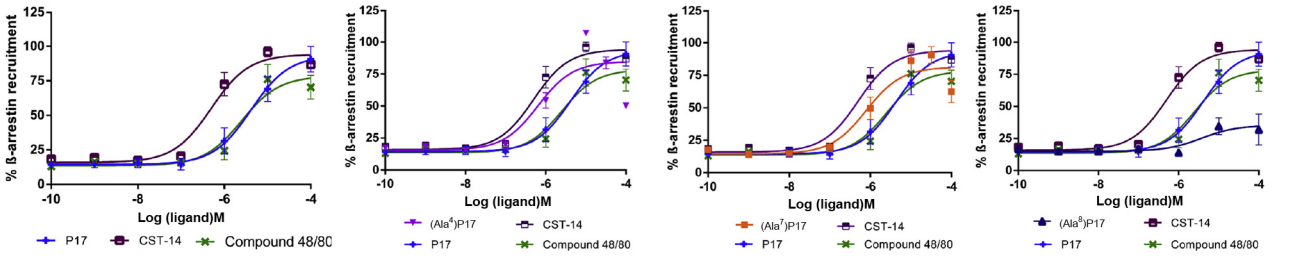

C

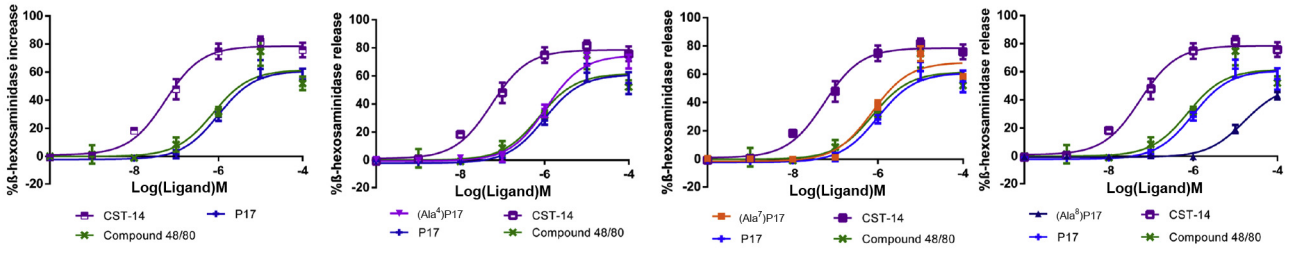

D

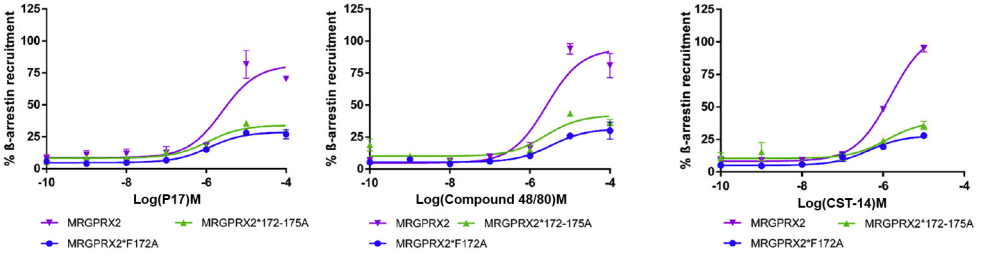

FIG 2. Locating the pharmacophore of peptide P17 and *in vitro* validation of peptide-receptor interaction site. **A**, Effect of single dose (10 µM) of P17 fragments on (**i**) β-arrestin recruitment and (**ii**) β-hexosaminidase release (percentage is compared with the basal). (**iii**) Superimposed MRGPRX2 receptor model in ribbon

MRGPRX2. MRGPRX2 gene knockdown was verified by qRT-PCR (see Fig E4, *A*i). In addition, pretreatment of quercetin (100 μM), an antagonist of MRGPRX2, significantly reduced stimulatory actions of both P17 and compound 48/80 in β-arrestin assay in HTLA (an HEK293 cell line stably expressing a tTA-dependent luciferase reporter and a β-arrestin2-TEV fusion gene) cells and β-hexosaminidase assays in wild-type LAD2 cells (Fig 1, *B*iii and iv).

Locating the pharmacophore region of peptide P17 using *in silico* 3-dimensional homology modeling and *in vitro* validation of peptide-receptor interaction site

To locate the pharmacophore region of P17, we first synthesized 8 P17 peptide fragments and determined their functional activities in both β-arrestin recruitment in receptor-transfected HTLA cells and β-hexosaminidase release assays in LAD2 cells (Fig 2, *A*i and ii). Our data suggest that P17 fragments 5-13 and 1-11, although less potent compared with the P17 whole peptide, significantly stimulated β-arrestin recruitment in receptor-transfected cells and degranulation of LAD2 cells. Thus, we initially speculated that the pharmacophore of P17 lay within the region 5-11 or 5-13. These data should allow more accurate prediction in *in silico* studies to locate MRGPRX2 aa residues important for ligand interactions.[45,46] In the meantime, we have also developed a 3-dimensional (3-D) model of MRGPRX2 using the homology modeling approach as previously published class A human pyroglutamylated RFamide peptide receptor and class B human secretin receptor.[47,48] Because MRGPRX2 is a class A orphan receptor structurally more related to opioid receptors, the 3-D model of MRGPRX2 was built using the κ-opioid receptor (PDB ID: 6B73) as a template.[49] Three different homology models were produced by SWISS-MODEL and MODELLER algorithms.[50] These models were then screened for steric collisions between atoms by the help of Ramachandran plot from Rampage server.[51] The final selected 3-D structure had 98.8% of aa residues in favored or allowed regions (see Fig E2, *A*i, in this article's Online Repository at www.jacionline.org). Visualization and verification of the receptor models were done by Schrodinger biological suite.[52] By Schrodinger Desmond, we were able to energy minimize the full receptor structure in the most thermodynamically stable conformation, which was then validated by virtual docking of a small compound agonist ZINC72453573 with known binding sites[53] on the receptor (Fig E2, *A*ii). In Fig 2, *A*iii, we show superimposed MRGPRX2 receptor model with ribbon structure docked with ZINC72453573 in ball and stick structure, P17 in yellow, $P17_{(5\text{-}11)}$ in blue, and $P17_{(5\text{-}13)}$ in gray. Finally, we have used MD simulation[54] for atomistic refinement to simulate molecular interactions of P17 fragments with MRGPRX2 in real time at 200 ns (see videos in this article's Online Repository at www.jacionline.org). Consolidated from both docking results of $P17_{(5\text{-}13)}$ and $P17_{(5\text{-}11)}$ (Fig 2, *A*iv; Fig E2, *A*iv) and MD (Fig E2, *B*), we predicted that P17 interacts with Tyr^{89}, Phe^{172}, Ser^{173}, Asp^{174}, Gly^{175}, Trp^{250}, Lys^{251}, and Ser^{253} residues of MRGPRX2. In particular, the Lys^{8} moiety of P17 specifically formed a cation-π interaction with Phe^{172} residue of MRGPRX2 (Fig 2, *A*iv).

Using *in silico* data as a reference, we tried to pinpoint specific interactions between P17 and MRGPRX2 by synthesizing a series of L-alanine–scanning mutants of P17, and consolidated their EC_{50} and E_{max} values (Fig 2, *A*v). For comparison purpose, we initially showed that P17 and 2 other positive controls, compound 48/48 and CST-14, recruited β-arrestin in MRGPRX2-transfected HTLA cells and stimulated β-hexosaminidase release in human LAD2 cells (Fig 2, *B* and *C*). Some P17-Ala scanning mutants such as [Ala^{1}]-, [Ala^{3}]-, [Ala^{5}]-, [Ala^{6}]-, [Ala^{9}]-, and [Ala^{13}] P17 exhibited no or less significant difference in both EC_{50} and E_{max} values in β-arrestin assay compared with P17 (Fig 2, *A*v; see Fig E3, *A*i, in this article's Online Repository at www.jacionline.org). However, alanine replacements at residues 4, 7, and 8 led to significant changes in EC_{50} values measured by β-arrestin assay ($P < .001$; Fig 2, *B* and *C*). Indeed, $Lys^{8} \rightarrow Ala^{8}$ substitution almost abolished its activity ($P < .0001$) as shown in Fig 2, *B* and *C*, whereas both $Glu^{4} \rightarrow Ala^{4}$ and $Glu^{7} \rightarrow Ala^{7}$ mutations resulted in slight enhancement in EC_{50} values in β-arrestin assay, indicating that these 2 mutant peptides are potentially more potent than P17 in activating the receptor (Fig 2, *B*). Finally, [Ala^{2}]-, [Ala^{10}]-, and [Ala^{12}]-substituted analogues also showed loss of activity in both β-arrestin and β-hexosaminidase assays to a lesser extent than [Ala^{8}]P17 (Fig E3, *A*ii and *B*). Thus, [Ala^{2}]-, [Ala^{8}]-, [Ala^{10}]-, and [Ala^{12}]-P17 acted as partial agonists. Interestingly, preincubation of wild-type LAD2 cells with [Ala^{8}]P17 (10 μM) drastically reduced the efficacy of P17 in both assays (Fig E3, *C*i and ii), suggesting that this point-substituted P17 analogue can be used as a competitive antagonist of the receptor. This observation has been reported in other partial and full agonist systems, where the partial agonist causes activation of a quiescent system and antagonism in a system activated by a more efficacious agonist.[55]

As we have predicted that residue Phe^{172} of MRGPRX2 formed a cation-π interaction with the Lys^{8} moiety of P17 and aa 172-175 might also be of importance, we have produced 2 site-directed mutants (MRGPRX2*F172A and MRGPRX2*172-175A) consisting of mutations at aa site 172 and another from 172 to 175 of MRGPRX2, for functional analyses. MRGPRX2 gene expression was verified by qRT-PCR (see Fig E4, *A*ii, in this article's Online Repository at www.jacionline.org). Both mutants displayed decreased activity in β-arrestin recruitment with P17 as well as with the 2 known agonists, compound 48/80 and CST-14 (Fig 2, *D*). Taken as a whole, these data were consistent with our *in silico* analysis that Lys^{8} of P17 and Phe^{172} of MRGPRX2

structure, docked with different agonistic molecules, that is, ZINC72453573 in ball and stick, P17(5-13) in gray, P17(5-11) in blue, and P17 in yellow. (**iv**) Docking of $P17_{(5\text{-}11)}$ showing the aa interactions with the receptor. (**v**) Effect of P17 fragments on both β-arrestin recruitment and β-hexosaminidase release assay consolidated as EC_{50} and % E_{max} values. **B,** Dose-response activation of Tango-MRGPRX2 construct with P17, [Ala^{4}]P17, [Ala^{8}]P17, and [Ala^{7}]P17 ($P \leq .0001$) (N = 3). **C,** Dose-response release of β-hexosaminidase in LAD2 cells with P17, [Ala^{4}]P17, [Ala^{8}]P17, and [Ala^{7}]P17 ($P \leq .0001$) (N = 3). **D,** Effect of P17, compound 48/80, and CST-14 on MRGPRX2 and MRGPRX2 mutant (MRGPRX2*F172A and MRGPRX2*172-175A) tango receptors in the β-arrestin recruitment assay ($P \leq .0001$) (N = 3). *ns*, Not significant. All values are means ± SEM (N = 3 or more and n = 3). Compound 48/80 and CST-14 are positive controls. ****$P \leq .0001$; ***$P \leq .001$; **$P \leq .01$; *$P \leq .05$; and ns $P > .05$.

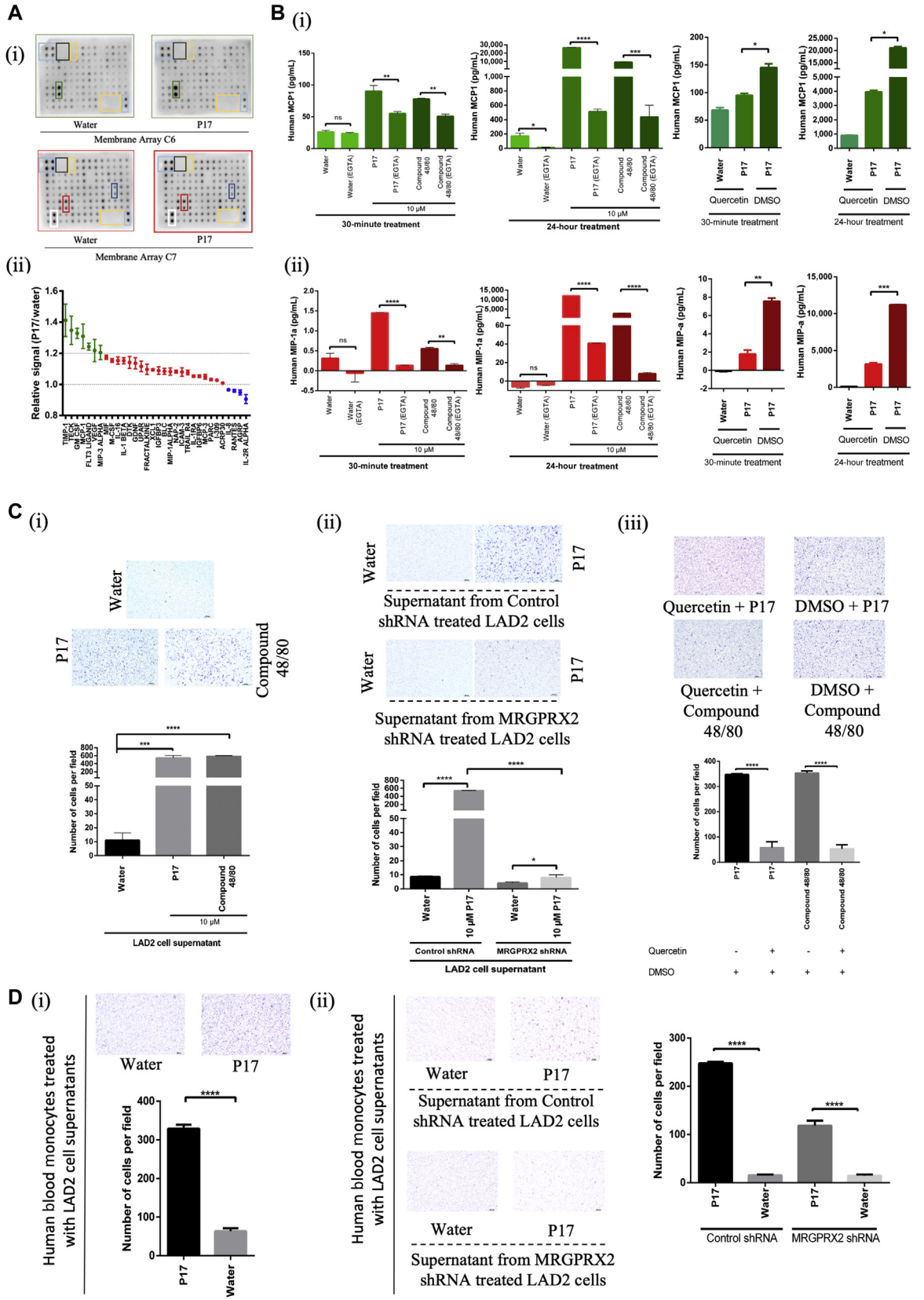

FIG 3. P17 induces release of cytokines in human LAD2 cells via MRGPRX2 and the subsequent recruitment of monocytes. **A,** Representative pictures showing the reactivity of cytokines released from LAD2 cells to the cytokine array (ab193656 – 120 targets, Abcam). **(i)** Membrane arrays with water and P17 treatment. Positive control (light blue boxes), blanks (yellow boxes), and negative control (black boxes). Representative colored

are key aa residues of the ligand/receptor complex responsible for the activation.

P17 induces release of cytokines in human LAD2 cells via MRGPRX2 and induces monocyte recruitment

To investigate the mechanisms of P17 in activation and degranulation of LAD2 cells, we screened for cytokine and chemokine release on 30-minute P17 (10 μM) stimulation using cytokine membrane arrays consisting of 120 different capture antibodies. We treated the membranes with water- or P17-treated LAD2 cell supernatants (Fig 3, *A*i). We displayed some representative hits with green, red, and white boxes in the array between controls and the treatments. The graph shows cytokine levels that are significantly different in comparison to controls (Fig 3, *A*ii). To validate these data, we selected 2 positive hits, monocyte chemoattractant protein 1 (MCP1) and macrophage inflammatory protein 1 α (MIP-1α), and measured their concentrations using ELISA after stimulation with water, P17, and compound 48/80, in addition to with or without ethylene glycol bis (2-aminoethyl ether) tetraacetic acid, a known calcium-chelating agent.[56] P17 and compound 48/80 induced MCP1 (Fig 3, *B*i) and MIP-1α (Fig 3, *B*ii) secretion in LAD2 cells (30 minutes and 24 hours). In addition, treatment of LAD2 cells with ethylene glycol bis (2-aminoethyl ether) tetraacetic acid (5 mM) before P17 and compound 48/80 administration significantly reduced the release of both cytokines. Moreover, quercetin (100 μM) treatment before P17 stimulation significantly abrogated cytokine release. In summary, these data suggest that P17-provoked cytokine release from MCs is mediated by MRGPRX2 via a calcium-dependent pathway.

As we noticed the release of cytokines such as MCP1[57-59] and MIP-1 α,[59,60] which are known to be chemoattractant for monocytes, we explored the effect of P17-treated LAD2 cell supernatant on monocyte recruitment using the standard transwell migration assay[57,61] as represented by the cartoon in Fig E5, *A*i, in this article's Online Repository at www.jacionline.org. The invaded cells were stained as depicted in Fig 3, *C*i, and counted using National Institutes of Health ImageJ software. Compared with the control group (water), treatment of LAD2 cells with 10 μM P17 or compound 48/80 yielded a supernatant that significantly enhanced the invasion capacities of THP-1 cells (Fig 3, *C*i). Similarly, supernatant from control shRNA-transduced LAD2 cells showed similar invasion capacities as untreated LAD2 cells (Fig 3, *C*ii). In contrast, MRGPRX2 shRNA-transduced LAD2 cell supernatant significantly reduced THP-1 invasion on P17 stimulation (Fig 3, *C*ii). Noteworthy, addition of 10 μM of P17 in LAD2-unconditioned culture medium had no effect on monocyte recruitment (Fig E5, *A*ii). In addition to the MRGPRX2 knockdown, we have investigated the effects of MRGPRX2 antagonist quercetin on P17- and compound 48/80-treatment of LAD2 cells. Quercetin significantly reduced both P17- and compound 48/80–mediated THP-1 monocyte recruitment (Fig 3, *C*iii). To study whether P17 can also induce human monocyte recruitment, we have isolated human monocytes from peripheral blood and performed the Transwell migration assay. The isolated human monocytes were validated beforehand using flow cytometry by double and single CD11b and/or CD14 staining (see Figs E6 and E7 in this article's Online Repository at www.jacionline.org), because human monocytes express both markers abundantly.[62-65] Similar to THP-1 cells, isolated human monocytes also showed significant P17-induced invasion capacity (Fig 3, *D*i). This migration is likely to be mediated by MRGPRX2 because MRGPRX2-impaired LAD2 cells recruited significantly less human monocytes than the wild-type LAD2 (Fig 3, *D*ii). Taken as a whole, these data suggest that P17-mediated monocyte recruitment is MC MRGPRX2-dependent.

P17-treated LAD2-MC line supernatant induces monocyte differentiation

In addition to monocyte recruitment abilities, some cytokines facilitate their differentiation. We determined the transcript levels of various macrophage markers on THP-1 cells in the presence of P17-treated LAD2 cell supernatant, and we found increased expression of cluster of differentiation 11a (CD11a), CD11b, cluster of differentiation 11c (CD11c), TNF-α, CD14, and intercellular adhesion molecule 1 (ICAM-1) (Fig 4, *A*i) in the same way as compound 48/80–conditioned supernatant. It should be noted that compound 48/80 *per se* increased TNF-α, CD14, and ICAM-1 transcripts and decreased CD11a transcripts in THP-1 monocytes. In addition, we have demonstrated that differentiation of THP-1 was MRGPRX2-dependent because pretreatment with quercetin (100 μM) affected P17-induced MC cytokine release, and subsequently lowered the differentiation-inducing transcripts in THP-1 monocytes (Fig 4, *A*ii). Our flow cytometry data indicate that P17-treated LAD2 cell supernatant induced the expression of monocyte differentiation marker CD11b in THP-1 cells (Fig 4, *B*; see Fig E8 in this article's Online Repository at www.jacionline.org). The photomicrographs showing the adhered THP-1 cells indicated that P17 induced cell differentiation because the nonadherent monocytes differentiated to adhere to the bottom of the wells (Fig 4, *C*i). The supernatant yielded from the P17-treated MRGPRX2 knocked-down LAD2 cells did not induce cell differentiation (Fig 4, *C*ii). These data

boxes indicate the location of the detection of cytokines, MCP1 (red), MIP-1α (green), IL2R- α (dark blue), and TMIP1 (white) (N = 2; data are pooled from 2 different individual experiments). (**ii**) Graph indicating only the significant fold change in reactivity of cytokine release (P17-treated/control) ($P < .05$). **B,** (**i**) MCP1 and (**ii**) MIP-1α secretion on P17 and compound 48/80 treatments for 30 minutes and 24 hours with and without EGTA (5 mM) and quercetin (100 μM) (N = 3). Values are means ± SD (N = 3 and n = 2). Representative images and the graph showing the migrated (THP-1 cells or human primary monocytes) cells through the membrane when they are treated with LAD2 cell supernatants. THP-1 migration in (**C**) (**i**) water, P17, and compound 48/80 treatment (N = 3), (**ii**) water and P17 treatment on control shRNA- and MRGPRX2 shRNA-transduced LAD2 cells (N = 3), and (**iii**) water and P17 treated with or without quercetin (N = 3). Human monocyte migration in (**D**) (**i**) water and P17 treatment and (**ii**) water and P17 treatment on control shRNA- and MRGPRX2 shRNA-transduced LAD2 cells (N=3). *DMSO*, Dimethyl sulfoxide; *EGTA*, ethylene glycol bis (2-aminoethyl ether) tetraacetic acid; *ns*, not significant. Values are mean ± SD (N = 3). $****P \leq .0001$; $***P \leq .001$; $**P \leq .01$; $*P \leq .05$; and ns $P > .05$.

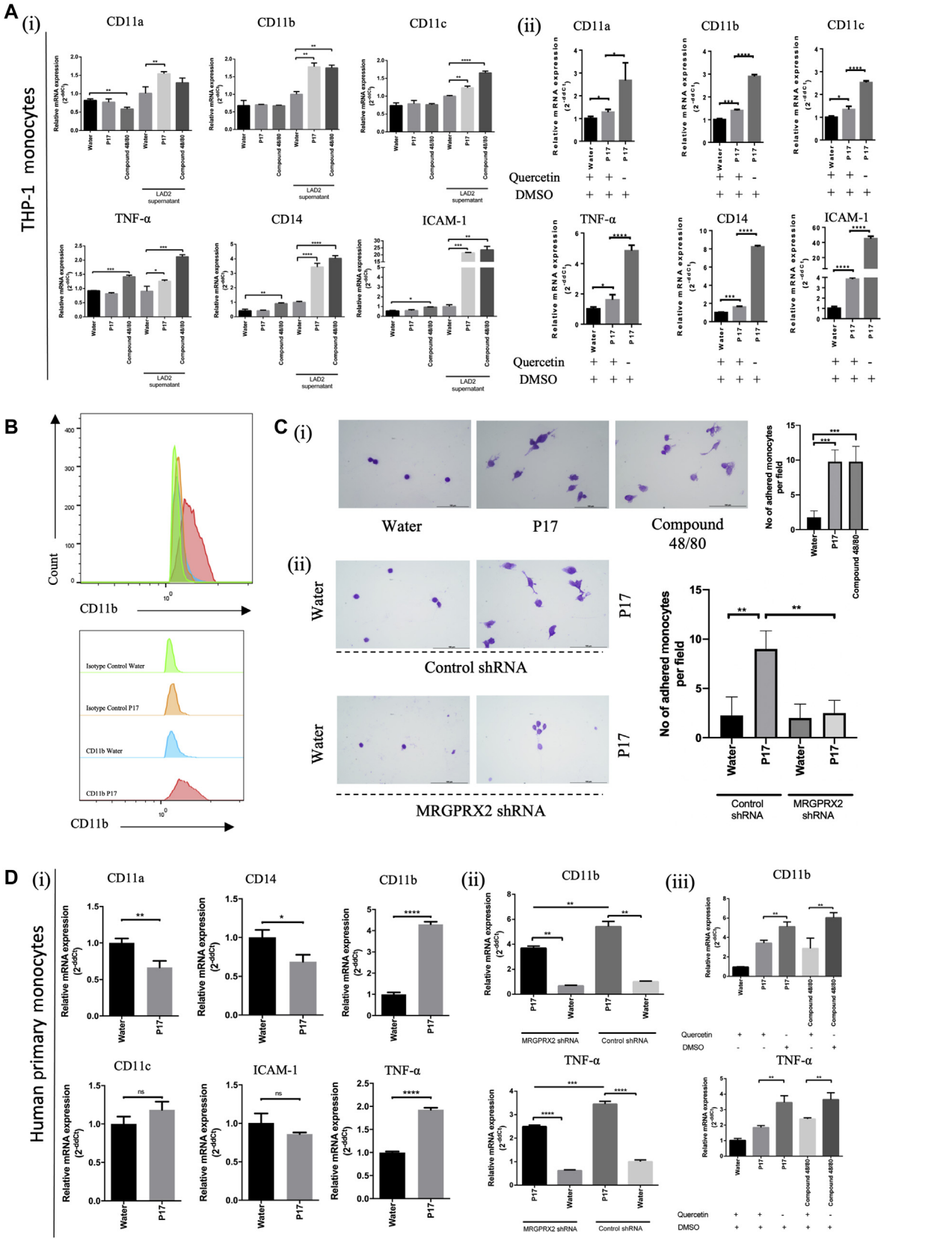

FIG 4. P17-treated MC supernatant induces monocyte differentiation. **A,** Surface markers were quantified using qRT-PCR for THP-1 monocytes differentiation into h-MDMs when incubated with LAD2 cell supernatants, (**i**) water, P17, and compound 48/80 with and without LAD2 cells, and (**ii**) in the presence of quercetin with water and P17. **B,** Flow cytometry graph showing the surface epitope, CD11b expression changes in the

demonstrate that the differentiation of THP-1 cells into monocyte-derived macrophages is mediated by MC MRGPRX2. Because the differentiated human monocytes showed elevated expression of CD11b and TNF-α (Fig 4, *D*i) but not CD11a, CD11c, CD14, and ICAM-I, we have picked CD11b and TNF-α for further analyses. The effects of P17 on CD11b and TNF-α transcript expression are MRGPRX2-dependent because MRGPRX2 knockdown significantly impaired their upregulation (Fig 4, *D*ii). We also subsequently showed that pretreatment with quercetin, before P17 or compound 48/80, lowered CD11b and TNF-α expression in differentiated human monocytes (Fig 4, *D*iii).

Effect of P17 in paw edema and vascular permeability through Evans blue extravasation assay and monocyte recruitment in mice ear

After showing that P17 induced MC activation and recruitment of monocytes, we sought to investigate the *in vivo* immunomodulatory actions of P17 in C57BL/6N mice by Evans blue extravasation and swelling, which are indicators of MC activation and inflammation due to the leakage of plasma from blood vessels.[30,34] We report that intraplantar administration of either P17 (10 μM) or CST-14 (10 μM) induced edema formation in the paws (Fig 5, *A*), whereas saline and secretin (10 μM), a negative control peptide (data not shown), did not. In addition, pretreatment with quercetin (100 μM) before P17 administration diminished plasma extravasation and paw edema (Fig 5, *B*). Quantification of plasma extravasation by Evans blue leakage and paw thickness are displayed in Fig 5, *B*. Both P17 and CST-14 increased paw edema and plasma extravasation, whereas quercetin (100 μM) decreased both paw edema and plasma extravasation when coadministrated with P17 or CST-14. Our data suggest that P17 induced MC activation *in vivo*, implying the recruitment of free circulating monocytes from the blood. To go further, we investigated monocyte recruitment in ears because MCs expressing MRGPRX2 are prevalent in ear tissues.[66,67] Intradermal injection of P17 in ear increased the inflammation because it causes local and controlled allergic reaction. Hematoxylin and eosin stain on the ear tissues showed significant increase in ear thickness on the P17-injected ears as compared with the saline control. In addition, quercetin significantly reduced the inflammation as the thickness of the tissue reduced when P17 is coadministered with quercetin (see Fig E9 in this article's Online Repository at www.jacionline.org). In addition, immunofluorescence and immunohistochemistry studies revealed that intradermal application of P17 in mice ear recruited $CD11b^+$ immune-cell population (green color in immunofluorescence and brown color in immunohistochemistry) 24 hours after injection, whereas cotreatment of P17 (10 μM) with quercetin (100 μM) abrogated this chemotactic effect (Fig 5, *C* and *D*). Migrated cells in immunohistochemistry were quantified with National Institutes of Health imageJ software and represented graphically in Fig 5, *D*. Because $CD11b^+$ immune-cell population could be monocytes or neutrophils, to further investigate the monocyte/macrophage infiltration, additionally, we have used macrophage marker F4/80 because it is one of the most commonly used marker for the identification of tissue macrophages[68-70] in the mouse ear.[71] Contrary to CD11b, neutrophils lack F4/80 protein at their surfaces[69,72] and F4/80 marker is often used to demonstrate monocyte infiltration in wound repair in mice models.[68] Thus, we have used both CD11b and F4/80 to double-stain the ear tissues by immunofluorescence. We showed that P17 intradermal injection in ear tissues stimulated infiltration of immune-cell population expressing CD11b and F4/80, whereas P17 treatment in the presence of quercetin reduced this process (Fig 5, *C*), as indicated by the mean fluorescence intensity quantified with Zeiss Zen microscope software, showing significant reductions in the intensity of $CD11b^+$ and $F4/80^+$ cells (see Fig E11 in this article's Online Repository at www.jacionline.org).

DISCUSSION

Hymenoptera venoms are composed of low-molecular-weight compounds such as biogenic amines, neurotoxic and cytotoxic peptides, and proteins, mostly enzymes that are major venom allergens. Ant stings are very frequent and manifest in various clinical symptoms including severe chest pain, nausea, severe sweating, loss of breath, serious swelling, fever, dizziness, and slurred speech. Anaphylactic shock is the most dramatic and occasionally fatal reaction.[73-75] Venom peptides target 2 predominant families of membrane-bound proteins, ion channels and GPCR, including neuropeptide GPCR.[15,76,77] For instance, peptides Pn3a from the tarantula *Pamphobeteus nigricolor*, MT7 from the green mamba *Dendroaspis angusticeps*, and $[Thr^6]$BK from the neotropical wasp *Polybia occidentalis* are ligands of voltage-gated sodium channel $Na_V1.7$, type-1 muscarinic, and type-2 bradykinin receptors, respectively.[78-80] Recently, we have deciphered the molecular diversity of the *T bicarinatum* ant venom, which encompasses 37 peptide precursors processed into several thousand peptides in the venom,[81] a source of structural templates for new therapeutics or bioactive agents. Bicarinalin, the most abundant peptide in *T bicarinatum* venom, is a broad-spectrum antimicrobial peptide,[11,82,83] whereas P17, the second most abundant peptide, does not display any antibacterial activity.[11] However, we previously reported that P17 induces an alternative phenotype of h-MDMs associated with an inflammatory response by activating an unknown GPCR. Broadening the knowledge on the mechanism of P17 action may contribute to the improvement of the treatment of immune-related diseases.

MRGPRX2 is a family member of Mas-related gene receptors. In humans, MRGPRX2 is mainly found in dorsal root ganglia (DRG), contributing to sleep regulation, locomotion, and cortical function after CST-14 binding.[84] However, MRGPRX2

LAD2 supernatant–treated cells. PE-conjugated IgG1kappa was used as the isotype control. **C,** Images and the graph showing the differentiated THP-1 cells incubated in the supernatant of (**i**) water, P17, and compound 48/80 and (**ii**) P17 treatment with MRGPRX2 shRNA-transduced and control shRNA-transduced LAD2 cells. **D,** (**i**) Surface markers were quantified using qRT-PCR for human primary monocyte differentiation when incubated with LAD2 cell supernatants (**i**) with water and P17. Surface marker expression when the supernatants were harvested from (**ii**) wild-type LAD2 and MRGPRX2-impaired LAD2 cells before water and/or P17 treatment and (**iii**) quercetin (100 μM) pretreated LAD2 cells before water and/or P17 treatment. *DMSO*, Dimethyl sulfoxide; *ns*, not significant. Values are means ± SD (N = 3 and n = 3). Compound 48/80 is used as a positive control. $^{****}P \leq .0001$; $^{***}P \leq .001$; $^{**}P \leq .01$; $^{*}P \leq .05$; and ns $P > .05$.

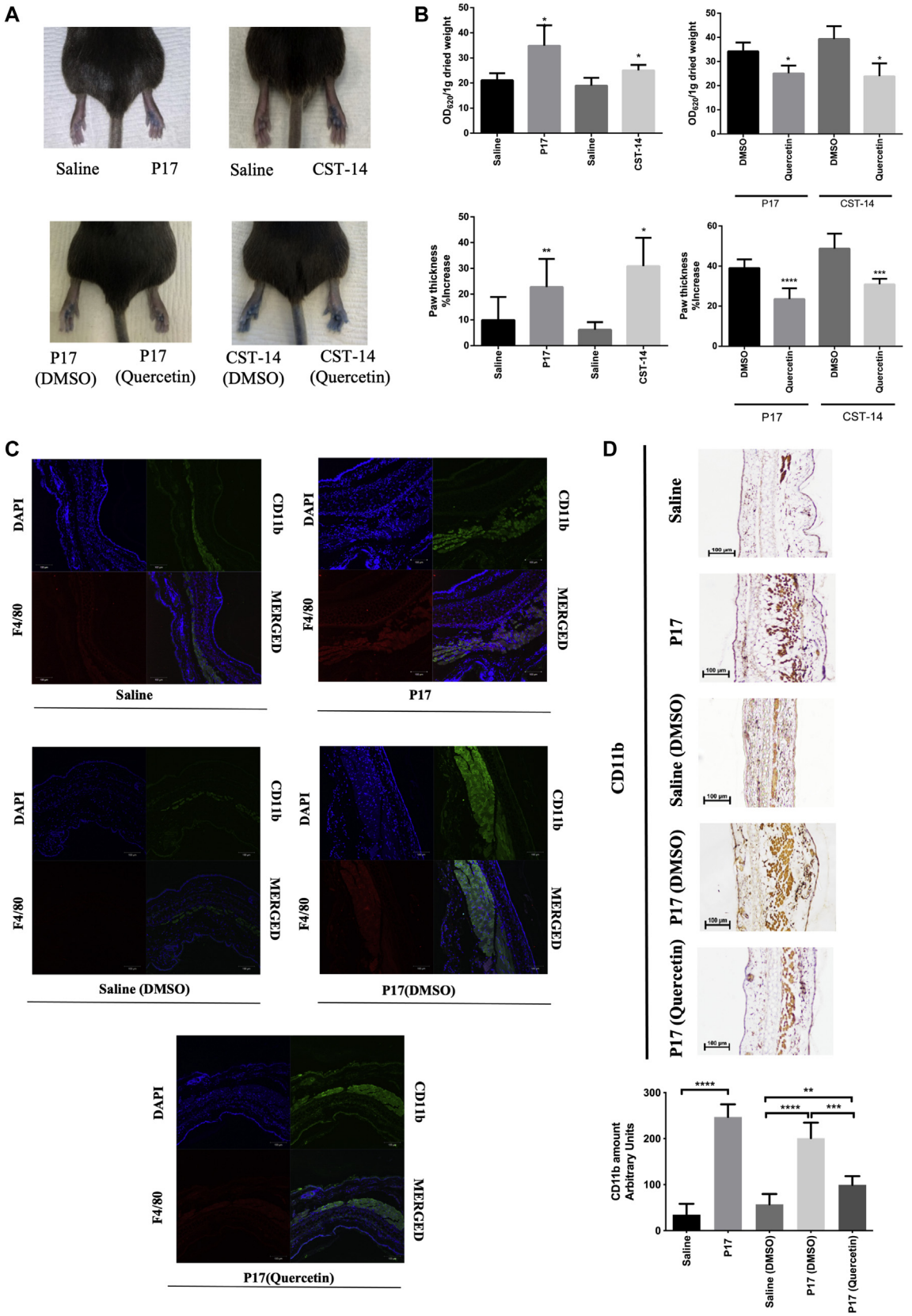

FIG 5. Effect of P17 in paw edema and vascular permeability through Evans blue extravasation assay and monocyte recruitment in mice ear. **A,** Wild-type mice injected with Evans blue through tail vein and intraplantar injection of P17 (10 μM, 5 μL in saline) and CST-14 (positive control) (10 μM, 5 μL in saline) in the left hind paw and 5 μL saline in the right hind paw; P17 and CST-14 with (right hind paw) and without

transcripts are also highly expressed in human MCs.[42] It is the only receptor in the MRGPR family to be expressed outside of the nervous system and being present in this connective tissue,[85,86] suggesting a function of this receptor in MC-neuron interaction to connect innate and nervous immune systems.[87] MCs are part of immune and neuroimmune systems acting as both effecter and immunomodulatory cells. A plethora of studies in the past decade have implicated MRGPRX2 in host defense, allergy, and inflammation.[42] It mediates the initiation of inflammation, angiogenesis, tissue remodeling, tissue injury–associated immune responses including innate or adaptive immune responses to pathogens as well as autoimmune disorders.[87,88] MC degranulation can be stimulated by either the classical IgE-dependent (high-affinity IgE receptor) pathway or alternatively the IgE-independent (MRGPRX2) pathway.[30,89,90] Both *in vitro* and *in vivo*, the classical and alternative activations show different patterns of MC degranulation that are associated with distinct local and systemic pathophysiological responses.[21] Therefore, it is essential to understand these mechanisms, particularly the alternative MC activation, which is an emerging concept and less understood. In this study, we have identified, from a panel of 314 GPCRs, MRGPRX2 as a first receptor for the ant venom peptide P17. Noteworthy, neither formyl peptide receptor–like 1 nor chemokine receptor 6 was activated by P17 in the Tango-GPCR screening. As a major GPCR involved in allergic responses,[91] MRGPRX2 is recognized for its responsivity toward a broad range of ligands that include various peptides and compounds such as CST-14, LL-37, substance P, mastoparan, and compound 48/80.[30,62,84,92-97] MRGPRX2 might have more than 1 binding pocket[98] involving multiple aa residues evidenced, for instance, by the following inactivating mutations: E164R(ECL2), G165E(ECL2), D184H(TM5), I225A(TM6), W243R(TM6), and H259Y(TM7) and Y279A(TM7).[90,98,99] Moreover, there are several Food and Drug Administration–approved drugs and antimicrobials that induce pseudoallergic responses via a common structural motif that could bind to MRGPRX2.[30,100] To decipher the interactions of P17 with MRGPRX2 and promote future agonist/antagonist design of specific ligands devoid of adverse effects,[30] we have built a 3-D model of MRGPRX2 by homology modeling followed by validation via a small compound agonist ZINC72453573 with known binding sites.[53] Importantly, we demonstrated that Lys^{8} of P17 is essential to interact with Phe^{172} in the ECL2 domain of MRGPRX2 via a cation-π interaction, and this was consistent with a battery of *in vitro* tests coupled to mutation analyses. More interestingly, some of the scanning mutants of P17 including [Ala^{8}]P17, [Ala^{4}]P17, and [Ala^{7}]P17 are functional antagonists and agonists and have the potential to be lead structures for future drug development in clinical usage. As we have mentioned before, hyperactivation of MCs by various allergens and envenomation leads to anaphylactic or anaphylactoid shock, which results in severe allergic reaction and even death.[73-75,101] Therefore, a peptide antagonist for MRGPRX2 might act as an antidote for anaphylaxis caused by envenomation.

Herein, we show that P17 stimulated the release of 7 cytokines (metallopeptidase inhibitor *1*, thymus-expressed chemokine, GM-CSF, MCP1, FLT3 ligand, vascular endothelial growth factor, and macrophage inflammatory protein 3 α) 1.2-fold more than control. Almost all of them are proinflammatory in nature, and some of them are known to be a potent chemoattractant for various immune cells. For example, MCP1[58,102] and MIP-1α[59,60] are 2 main chemokines involved in monocyte recruitment. Our data, particularly the *in vitro* and *ex vivo* finding, collectively suggest that P17 via MRGPRX2 stimulated LAD2 cytokine releases and concomitantly recruited monocytes and then differentiated them into proinflammatory-type (M1-type) h-MDMs. This was validated by the release of cytokines (GM-CSF and macrophage-CSF)[103,104] and expressions of CD11a, CD11b, CD11c, CD14, TNF-α, and ICAM-1 marker genes.[105-110] MCs are known to play a major role in innate immunity by releasing various cytokines via either high-affinity IgE receptor or MRGPRX2.[30,89] In a very recent study, MRGPRX2 has been shown to recruit neutrophils[62] and monocytes,[63] and the MRGPRX2 agonist, LL-37, also recruits neutrophils via formyl peptide receptor–like 1 activation.[111,112] However, to our knowledge, MRGPRX2-mediated concomitant monocyte recruitment and differentiation has not been previously reported or demonstrated. Monocytes can be differentiated into inflammatory or anti-inflammatory subset on the basis of the environment. On infection or tissue damage, they could infiltrate the tissues to differentiate into either macrophages or dendritic cells (DCs), which are morphologically distinct from each other; macrophages and DCs are defined as $F4/80^{+}$ and $CD11c^{+}$-positive cells, respectively.[113,114]

In this study, we demonstrate that a novel peptide from ant venom activates MRGPRX2 in a Ca^{2+}-dependent manner on MCs to recruit monocytes, but also differentiates them into an $CD11b^{+}$ and $F4/80^{+}$ immune population, possibly into macrophages. It is plausible that there is more than 1 immune-cell population at the P17-injected site in *in vivo* models because neutrophils are known to be recruited by MRGPRX2 activation.[62] However, in this study, we focused on the monocyte recruitment because our *in vitro* finding suggests monocyte recruitment and differentiation. Regardless of the ambiguity in the immune-cell population being recruited, this study shows that P17 is a potent MRGPRX2 agonist that induces monocyte recruitment and differentiation via activating MCs. Mice Mas-related G protein–coupled receptor-B2 is the human orthologue of MRGPRX2.[30] It is to be noted that findings in this study are limited to the *in vitro*, *ex vivo*, and *in vivo* studies carried out. Validation of these findings in Mas-related G protein–coupled receptor-B2 knockout mice model will enhance our current

(left hind paw) quercetin (100 μM) (N = 6). **B,** Extravasated paws were quantified for Evans blue leakage and paw edema (N = 6). Evans blue leakage and paw edema with agonists and saline treatment and/or in the presence of quercetin pretreatment (100 μM). **C,** Mouse ears intradermal injection (N = 6/group) for 24 hours with P17 (10 μM), saline, saline (DMSO), P17 (DMSO), and P17 (10 μM) cotreated with quercetin (100 μM). Tissue sections were stained with CD11b (green), macrophage marker F4/80 (red), and DAPI (blue) before observation under a Carl Zeiss LSM 710 NLO microscope. **D,** CD11b immunohistochemical staining of tissue sections using Leica BOND-MAX machine and imaged under Nikon Eclipse Ni-U upright microscope (Nikon H550L). Recruited cells with CD11b marker are quantified with National Institutes of Health ImageJ software. *DAPI*, 4′-6-Diamidino-2-phenylindole, dihydrochloride; *DMSO*, dimethyl sulfoxide. Values are means ± SD (N = 6 per group). $****P \leq .0001$; $***P \leq .001$; $**P \leq .01$.

understanding of MRGPRX2-mediated responses via P17 activation. In addition, the study reveals key structural information of the receptor, which in turn can be used to target novel therapeutic drugs that could be used for inflammatory, allergic, or allergic-related diseases. Overall, these data suggest that P17 or agonists of MRGPRX2 could activate MCs to induce allergic and inflammatory responses through MRGPRX2 and modulate the microenvironments by concurrently recruiting and differentiating monocytes in the tissues. Our data also compel us to revisit various pathophysiological conditions mediated by the MRGPRX2-MCs axis. With the given structural insights and the novel immunomodulatory pathway, MRGPRX2 could be a major therapeutic target to modulate the microenvironment in various autoimmune and inflammatory disorders, particularly in the gut. As mentioned above, various cytokines/chemokines that are released on P17 treatment are already known as key players in inflammatory bowel disease and colorectal cancer. For example, thymus-expressed chemokine is a potent chemoattractant for cells expressing IgA antibody-secreting cells to intestine,[115] macrophage migration inhibitory factor is an important factor at the intestinal barrier,[116] and neutrophil-activating protein 2 recruits mesenchymal stem cells for tissue repair and wound healing.[117,118] Other studies report the protective effect of MRGPRX2 ligands such as CST-14[119,120] and protegrin[121,122] in Dextran sodium sulfate (DSS)-induced colitis, a heavily explored aspect of MCs. However, colon is known to contain a nervous system of its own, sensitive to known MRPGRX2 agonists such as CST-14, substance P, and vasoactive intestinal peptide.[123] Therefore, MRGPRX2 possibly can be the intermediary link between the nervous system and colon. In addition, the enteric nervous system is innervated by 3 types of sensory neurons: DRG, nodose/jugular ganglia, and intrinsic primary afferent neurons.[123,124] Not to mention, MRGPRX2 is also highly expressed in DRG.[84] It is therefore plausible that these ligands pose a protective effect through MRGPRX2, which in turn modulate the microenvironment via cytokines and DRG in inflammatory bowel disease or colorectal cancer. Exploiting the MRGPRX2-MCs-enteric nervous system axis will surely enhance our current understanding on intestinal immunity and intestinal inflammatory processes.

In this study, we identified that P17 acted through MRGPRX2. In our previous studies, we demonstrated that P17 directly activates h-MDMs via an unknown GPCR and induces an alternative/anti-inflammatory phenotype of h-MDMs (M2 type).[12] The major question that rises up is whether P17 acts through MRGPRX2 in h-MDMs, although its expression in these cells is relatively low compared with MCs (see Fig E10, *Ai*, in this article's Online Repository at www.jacionline.org).[125] P17 was able to induce $[Ca^{2+}]_i$ in THP-1 only at very high concentration (Fig E10, *Aii*). It has to be noted that M1 and M2 types are an oversimplified characterization of macrophages because they are known to be very complex.[126] The cytokines released on P17 activation in LAD2 cells are mainly proinflammatory cytokines that are known to induce M1 macrophage polarization.[127] In addition, LAD2 cells–induced h-MDMs have shown an increase in markers that correspond to M1-type macrophage such as ICAM-1, CD11b, and CD11c hallmarks of M1-type macrophages.[101,128,129] However, we showed that LAD2 cells–induced h-MDMs displayed a marked increase in the expression of CD11b marker, whereas direct activation of h-MDMs with P17 showed a reduction in CD11b.[12] Thus, there is a possibility that there is more than 1 GPCR that can be activated by P17 in different immune cells. It is likely that P17 activates LAD2 cells via MRGPRX2 to recruit monocytes and differentiate them into M1-type h-MDMs, and subsequently via an unknown GPCR directly activating h-MDMs to induce the M2-type h-MDMs for pathogen clearing, as we have previously reported.[12] Therefore, an extensive study on this aspect should be carried out in the future to further understand the detailed mechanism of P17 in various immune cells and their interconnectivity in their immunomodulatory effect.

We acknowledge Lau H.Y. Alaster (The Chinese University of Hong Kong, Hong Kong SAR) for providing LAD-2 cells, Leo T.O. Lee (University of Macau, Taipa, Macau, China) for PRESTO-tango screening system and HTLA cells, and Miss Do Ye Lim and Miss Carmen Ng for their assistance with some experiments.

Key messages

- **P17 activates MRGPRX2 in MCs.**
- **Residues Lys^{8} of P17 and Phe^{172} of MRGPRX2 are crucial for the ligand/receptor interaction.**
- **P17 recruits and differentiates monocytes via MRGPRX2 activation in MCs.**

REFERENCES

1. Lewis RJ, Garcia ML. Therapeutic potential of venom peptides. Nat Rev Drug Discov 2003;2:790-802.
2. Pennington MW, Czerwinski A, Norton RS. Peptide therapeutics from venom: current status and potential. Bioorganic Med Chem 2018;26:2738-58.
3. Zasloff M. Antimicrobial peptides of multicellular organisms. Nature 2002;415:389.
4. Gupta S, Bhatia G, Sharma A, Saxena S. Host defense peptides: an insight into the antimicrobial world. J Oral Maxillofacial Pathol 2018;22:239.
5. Soehnlein O, Kai-Larsen Y, Frithiof R, Sorensen OE, Kenne E, Scharffetter-Kochanek K, et al. Neutrophil primary granule proteins HBP and HNP1–3 boost bacterial phagocytosis by human and murine macrophages. J Clin Investig 2008;118:3491-502.
6. Niyonsaba F, Iwabuchi K, Someya A, Hirata M, Matsuda H, Ogawa H, et al. A cathelicidin family of human antibacterial peptide LL-37 induces mast cell chemotaxis. Immunology 2002;106:20-6.
7. Yang D, Chen Q, Schmidt AP, Anderson GM, Wang JM, Wooters J, et al. LL-37, the neutrophil granule–and epithelial cell–derived cathelicidin, utilizes formyl peptide receptor–like 1 (FPRL1) as a receptor to chemoattract human peripheral blood neutrophils, monocytes, and T cells. J Exp Med 2000;192:1069-74.
8. Heilborn JD, Nilsson MF, Sørensen O, Ståhle-Bäckdahl M, Kratz G, Weber G, et al. The cathelicidin anti-microbial peptide LL-37 is involved in re-epithelialization of human skin wounds and is lacking in chronic ulcer epithelium. J Investig Dermatol 2003;120:379-89.
9. Koczulla R, Von Degenfeld G, Kupatt C, Krötz F, Zahler S, Gloe T, et al. An angiogenic role for the human peptide antibiotic LL-37/hCAP-18. J Clin Investig 2003;111:1665-72.
10. Devine DA, Hancock RE. Mammalian host defense peptides. Cambridge, UK: Cambridge University Press; 2004.
11. Rifflet A, Gavalda S, Téné N, Orivel J, Leprince J, Guilhaudis L, et al. Identification and characterization of a novel antimicrobial peptide from the venom of the ant *Tetramorium bicarinatum*. Peptides 2012;38:363-70.
12. Benmoussa K, Authier H, Prat M, AlaEddine M, Lefèvre L, Rahabi MC, et al. P17, an original host defense peptide from ant venom, promotes antifungal activities of macrophages through the induction of C-type lectin receptors dependent on LTB4-mediated PPARγ activation. Front Immunol 2017;8:1650.
13. Pierce KL, Premont RT, Lefkowitz RJ. Seven-transmembrane receptors. Nat Rev Mol Cell Biol 2002;3:639-50.
14. Hauser AS, Attwood MM, Rask-Andersen M, Schiöth HB, Gloriam DE. Trends in GPCR drug discovery: new agents, targets and indications. Nat Rev Drug Discov 2017;16:829-42.

15. Muratspahić E, Freissmuth M, Gruber CW. Nature-derived peptides: a growing niche for GPCR ligand discovery. Trends Pharmacol Sci 2019;40:309-26.
16. On JS, Duan C, Chow BK, Lee LT. Functional pairing of class B1 ligand-GPCR in cephalochordate provides evidence of the origin of PTH and PACAP/glucagon receptor family. Mol Biol Evolution 2015;32:2048-59.
17. Basith S, Cui M, Macalino SJ, Park J, Clavio NA, Kang S, et al. Exploring G protein-coupled receptors (GPCRs) ligand space via cheminformatics approaches: impact on rational drug design. Front Pharmacol 2018;9:128.
18. Tilley DG. G protein–dependent and G protein–independent signaling pathways and their impact on cardiac function. Circ Res 2011;109:217-30.
19. W Gruber C, Muttenthaler M, Freissmuth M. Ligand-based peptide design and combinatorial peptide libraries to target G protein-coupled receptors. Curr Pharm Des 2010;16:3071-88.
20. Wacker D, Stevens RC, Roth BL. How ligands illuminate GPCR molecular pharmacology. Cell 2017;170:414-27.
21. Gaudenzio N, Sibilano R, Marichal T, Starkl P, Reber LL, Cenac N, et al. Different activation signals induce distinct mast cell degranulation strategies. J Clin Investig 2016;126:3981-98.
22. Tatemoto K, Nozaki Y, Tsuda R, Kaneko S, Tomura K, Furuno M, et al. Endogenous protein and enzyme fragments induce immunoglobulin E-independent activation of mast cells via a G protein-coupled receptor, MRGPRX 2. Scand J Immunol 2018;87:e12655.
23. Ferry X, Eichwald V, Daeffler L, Landry Y. Activation of βγ subunits of Gi2 and Gi3 proteins by basic secretagogues induces exocytosis through phospholipase Cβ and arachidonate release through phospholipase Cγ in mast cells. J Immunol 2001;167:4805-13.
24. Ciancetta A, Sabbadin D, Federico S, Spalluto G, Moro S. Advances in computational techniques to study GPCR–ligand recognition. Trends Pharmacol Sci 2015;36:878-90.
25. Thapaliya M, Ayudhya CCN, Amponnawarat A, Roy S, Ali H. Mast cell-specific MRGPRX2: a key modulator of neuro-immune interaction in allergic diseases. Curr Allergy Asthma Rep 2021;21:1-11.
26. Kim HS, Kawakami Y, Kasakura K, Kawakami T. Recent advances in mast cell activation and regulation. F1000Research 2020;9.
27. Babina M. The pseudo-allergic/neurogenic route of mast cell activation via MRGPRX2: discovery, functional programs, regulation, relevance to disease, and relation with allergic stimulation. Itch 2020;5:e32.
28. Reinholz M, Ruzicka T, Schauber J. Cathelicidin LL-37: an antimicrobial peptide with a role in inflammatory skin disease. Ann Dermatol 2012;24:126-35.
29. Muto Y, Wang Z, Vanderberghe M, Two A, Gallo RL, Di Nardo A. Mast cells are key mediators of cathelicidin-initiated skin inflammation in rosacea. J Investig Dermatol 2014;134:2728-36.
30. McNeil BD, Pundir P, Meeker S, Han L, Undem BJ, Kulka M, et al. Identification of a mast-cell-specific receptor crucial for pseudo-allergic drug reactions. Nature 2015;519:237.
31. Lansu K, Karpiak J, Liu J, Huang X-P, McCorvy JD, Kroeze WK, et al. In silico design of novel probes for the atypical opioid receptor MRGPRX2. Nat Chem Biol 2017;13:529.
32. Kumar M, Singh K, Duraisamy K, Allam AA, Ajarem J, Kwok Chong Chow B. Protective effect of genistein against compound 48/80 induced anaphylactoid shock via inhibiting MAS related G protein-coupled receptor X2 (MRGPRX2). Molecules 2020;25:1028.
33. Schmittgen TD, Livak KJ. Analyzing real-time PCR data by the comparative CT method. Nat Protoc 2008;3:1101-8.
34. Liu R, Che D, Zhao T, Pundir P, Cao J, Lv Y, et al. MRGPRX2 is essential for sinomenine hydrochloride induced anaphylactoid reactions. Biochem Pharmacol 2017;146:214-23.
35. Subramanian H, Gupta K, Lee D, Bayir AK, Ahn H, Ali H. β-Defensins activate human mast cells via Mas-related gene X2. J Immunol 2013;191:345-52.
36. Eustache S, Leprince J, Tufféry P. Progress with peptide scanning to study structure-activity relationships: the implications for drug discovery. Expert Opin Drug Discov 2016;11:771-84.
37. Touchard A, Aili SR, Téné N, Barassé V, Klopp C, Dejean A, et al. Venom peptide repertoire of the European myrmicine ant *Manica rubida*: identification of insecticidal toxins. J Proteome Res 2020;19:1800-11.
38. Meital LT, Coward AS, Windsor MT, Bailey TG, Kuballa A, Russell FD. A simple and effective method for the isolation and culture of human monocytes from small volumes of peripheral blood. J Immunol Methods 2019;472:75-8.
39. Ou Y-Q, Chen L-H, Li X-J, Lin Z-B, Li W-D. Sinomenine influences capacity for invasion and migration in activated human monocytic THP-1 cells by inhibiting the expression of MMP-2, MMP-9, and CD147. Acta Pharmacol Sinica 2009;30:435-41.
40. Mak SO, Zhang L, Chow BK. In vivo actions of SCTR/AT1aR heteromer in controlling Vp expression and release via cFos/cAMP/CREB pathway in magnocellular neurons of PVN. FASEB J 2019;33:5389-98.
41. Lafleur MA, Werner J, Fort M, Lobenhofer EK, Balazs M, Goyos A. MRGPRX2 activation as a rapid, high-throughput mechanistic-based approach for detecting peptide-mediated human mast cell degranulation liabilities. J Immunotoxicol 2020;17:110-21.
42. Subramanian H, Gupta K, Ali H. Roles of Mas-related G protein–coupled receptor X2 on mast cell–mediated host defense, pseudoallergic drug reactions, and chronic inflammatory diseases. J Allergy Clin Immunol 2016;138:700-10.
43. Alkanfari I, Freeman KB, Roy S, Jahan T, Scott RW, Ali H. Small-molecule host-defense peptide mimetic antibacterial and antifungal agents activate human and mouse mast cells via mas-related GPCRs. Cells 2019;8:311.
44. Ding Y, Che D, Li C, Cao J, Wang J, Ma P, et al. Quercetin inhibits Mrgprx2-induced pseudo-allergic reaction via PLCγ-IP3R related Ca2+ fluctuations. Int Immunopharmacol 2019;66:185-97.
45. Ciemny M, Kurcinski M, Kamel K, Kolinski A, Alam N, Schueler-Furman O, et al. Protein–peptide docking: opportunities and challenges. Drug Discov Today 2018;23:1530-7.
46. Diharce J, Cueto M, Beltramo M, Aucagne V, Bonnet P. In silico peptide ligation: iterative residue docking and linking as a new approach to predict protein-peptide interactions. Molecules 2019;24:1351.
47. Singh K, Senthil V, Arokiaraj AW, Leprince J, Lefranc B, Vaudry D, et al. Structure-activity relationship studies of N- and C-terminally modified secretin analogs for the human secretin receptor. PLoS One 2016;11:e0149359.
48. Neveu C, Dulin F, Lefranc B, Galas L, Calbrix C, Bureau R, et al. Molecular basis of agonist docking in a human GPR 103 homology model by site-directed mutagenesis and structure–activity relationship studies. Br J Pharmacol 2014;171:4425-39.
49. Che T, Majumdar S, Zaidi SA, Ondachi P, McCorvy JD, Wang S, et al. Structure of the nanobody-stabilized active state of the kappa opioid receptor. Cell 2018;172:55-67.e15.
50. Webb B, Sali A. Comparative protein structure modeling using MODELLER. Curr Protoc Bioinformatics 2014;47:5.6.1-32.
51. Lovell SC, Davis IW, Arendall WB III, de Bakker PI, Word JM, Prisant MG, et al. Structure validation by Calpha geometry: phi, psi and Cbeta deviation. Proteins 2003;50:437-50.
52. Zhu K, Day T, Warshaviak D, Murrett C, Friesner R, Pearlman D. Antibody structure determination using a combination of homology modeling, energy-based refinement, and loop prediction. Proteins 2014;82:1646-55.
53. Kim S, Thiessen PA, Bolton EE, Chen J, Fu G, Gindulyte A, et al. PubChem Substance and Compound databases. Nucleic Acids Res 2016;44:D1202-13.
54. Lupala CS, Rasaeifar B, Gomez-Gutierrez P, Perez JJ. Using molecular dynamics for the refinement of atomistic models of GPCRs by homology modeling. J Biomol Struct Dyn 2018;36:2436-48.
55. Negus SS. Some implications of receptor theory for in vivo assessment of agonists, antagonists and inverse agonists. Biochemical pharmacology 2006;71(12):1663-70.
56. Bai J, Duraisamy K, Mak SO, Allam A, Ajarem J, Li Z, et al. Role of SCTR/AT1aR heteromer in mediating ANGII-induced aldosterone secretion. PLoS One 2019;14:e0222005.
57. Danella Polli C, Alves Toledo K, Franco LH, Sammartino Mariano V, de Oliveira LL, Soares Bernardes E, et al. Monocyte migration driven by galectin-3 occurs through distinct mechanisms involving selective interactions with the extracellular matrix. ISRN Inflamm 2013;2013.
58. Deshmane SL, Kremlev S, Amini S, Sawaya BE. Monocyte chemoattractant protein-1 (MCP-1): an overview. J Interferon Cytokine Res 2009;29:313-26.
59. Göser S, Öttl R, Brodner A, Dengler TJ, Torzewski J, Egashira K, et al. Critical role for monocyte chemoattractant protein-1 and macrophage inflammatory protein-1α in induction of experimental autoimmune myocarditis and effective anti–monocyte chemoattractant protein-1 gene therapy. Circulation 2005;112:3400-7.
60. DiPietro LA, Burdick M, Low QE, Kunkel SL, Strieter RM. MIP-1alpha as a critical macrophage chemoattractant in murine wound repair. J Clin Investig 1998;101:1693-8.
61. Wang G, Zhao H, Zheng B, Yuan Y, Han Q, Tian Z, et al. TLR2 promotes monocyte/macrophage recruitment into the liver and microabscess formation to limit the spread of *Listeria monocytogenes*. Front Immunol 2019;10:1388.
62. Arifuzzaman M, Mobley YR, Choi HW, Bist P, Salinas CA, Brown ZD, et al. MRGPR-mediated activation of local mast cells clears cutaneous bacterial infection and protects against reinfection. Sci Adv 2019;5:eaav0216.
63. Green DP, Limjunyawong N, Gour N, Pundir P, Dong X. A mast-cell-specific receptor mediates neurogenic inflammation and pain. Neuron 2019;101:412-20.e3.

64. Wong S-C, Ong S-M, Teng K, Newell E, Chen H, Chen J, et al. A novel, five-marker alternative to CD16-CD14 gating to identify the three human monocyte subsets. Front Immunol 2019;10:1761.
65. Kapellos TS, Bonaguro L, Gemünd I, Reusch N, Saglam A, Hinkley ER, et al. Human monocyte subsets and phenotypes in major chronic inflammatory diseases. Front Immunol 2019;10:2035.
66. Mencarelli A, Gunawan M, Yong KSM, Bist P, Tan WWS, Tan SY, et al. A humanized mouse model to study mast cells mediated cutaneous adverse drug reactions. J Leukoc Biol 2020;107:797-807.
67. Yamada K, Sato H, Sakamaki K, Kamada M, Okuno Y, Fukuishi N, et al. Suppression of IgE-independent degranulation of murine connective tissue-type mast cells by dexamethasone. Cells 2019;8:112.
68. Crane MJ, Daley JM, van Houtte O, Brancato SK, Henry WL Jr, Albina JE. The monocyte to macrophage transition in the murine sterile wound. PLoS One 2014;9:e86660.
69. Dunay IR, Fuchs A, Sibley LD. Inflammatory monocytes but not neutrophils are necessary to control infection with *Toxoplasma gondii* in mice. Infect Immun 2010;78:1564-70.
70. Gordon S, Plüddemann A. Tissue macrophages: heterogeneity and functions. BMC Biol 2017;15:53.
71. Lang H, Nishimoto E, Xing Y, Brown LN, Noble KV, Barth JL, et al. Contributions of mouse and human hematopoietic cells to remodeling of the adult auditory nerve after neuron loss. Mol Ther 2016;24:2000-11.
72. Waddell LA, Lefevre L, Bush SJ, Raper A, Young R, Lisowski ZM, et al. ADGRE1 (EMR1, F4/80) is a rapidly-evolving gene expressed in mammalian monocyte-macrophages. Front Immunol 2018;9:2246.
73. Fitzgerald KT, Flood AA. Hymenoptera stings. Clin Tech Small Anim Pract 2006;21:194-204.
74. Ryan KC, Caravati EM. Life-threatening anaphylaxis following envenomation by two different species of Crotalidae. J Wilderness Med 1994;5:263-8.
75. Golden DB. Insect sting anaphylaxis. Immunol Allergy Clin North Am 2007;27:261-72.
76. Mendel HC, Kaas Q, Muttenthaler M. Neuropeptide signalling systems—an underexplored target for venom drug discovery. Biochem Pharmacol 2020;181:114129.
77. Cardoso FC. Multi-targeting sodium and calcium channels using venom peptides for the treatment of complex ion channels-related diseases. Biochem Pharmacol 2020;181:114107.
78. Deuis JR, Dekan Z, Wingerd JS, Smith JJ, Munasinghe NR, Bhola RF, et al. Pharmacological characterisation of the highly Na V 1.7 selective spider venom peptide Pn3a. Sci Rep 2017;7:40883.
79. Mortari M, Cunha A, Carolino R, Coutinho-Netto J, Tomaz J, Lopes N, et al. Inhibition of acute nociceptive responses in rats after icv injection of Thr6-bradykinin, isolated from the venom of the social wasp, *Polybia occidentalis*. Br J Pharmacol 2007;151:860-9.
80. Max SI, Liang J-S, Potter LT. Purification and properties of m1-toxin, a specific antagonist of m1 muscarinic receptors. J Neurosci 1993;13:4293-300.
81. Touchard A, Téné N, Song PCT, Lefranc B, Leprince Jrm, Treilhou M, et al. Deciphering the molecular diversity of an ant venom peptidome through a venomics approach. J Proteome Res 2018;17:3503-16.
82. Téné N, Roche-Chatain V, Rifflet A, Bonnafé E, Lefranc B, Leprince J, et al. Potent bactericidal effects of bicarinalin against strains of the Enterobacter and Cronobacter genera. Food Control 2014;42:202-6.
83. Téné N, Bonnafé E, Berger F, Rifflet A, Guilhaudis L, Ségalas-Milazzo I, et al. Biochemical and biophysical combined study of bicarinalin, an ant venom antimicrobial peptide. Peptides 2016;79:103-13.
84. Robas N, Mead E, Fidock M. MrgX2 is a high potency cortistatin receptor expressed in dorsal root ganglion. J Biol Chem 2003;278:44400-4.
85. Bader M, Alenina N, Andrade-Navarro MA, Santos RA. Mas and its related G protein–coupled receptors. Mrgprs. Pharmacol Rev 2014;66:1080-105.
86. Carstens E, Akiyama T. Itch: mechanisms and treatment. Boca Raton (FL): CRC Press/Taylor & Francis; 2014.
87. Lu L, Kulka M, Unsworth LD. Peptide-mediated mast cell activation: ligand similarities for receptor recognition and protease-induced regulation. J Leukocyte Biol 2017;102:237-51.
88. Tsai M, Grimbaldeston M, Galli SJ. Mast cells and immunoregulation/immunomodulation. In: Mast cell biology. Springer; 2011. pp. 186-211.
89. Karhu T, Akiyama K, Vuolteenaho O, Bergmann U, Naito T, Tatemoto K, et al. Mast cell degranulation via MRGPRX2 by isolated human albumin fragments. Biochim Biophys Acta 2017;1861:2530-4.
90. Chompunud Na Ayudhya C, Roy S, Alkanfari I, Ganguly A, Ali H. Identification of gain and loss of function missense variants in MRGPRX2's transmembrane and intracellular domains for mast cell activation by substance P. Int J Mol Sci 2019;20:5247.
91. Porebski G, Kwiecien K, Pawica M, Kwitniewski M. Mas-related G protein-coupled receptor-X2 (MRGPRX2) in drug hypersensitivity reactions. Front Immunol 2018;9:3027.
92. Ferry X, Brehin S, Kamel R, Landry Y. G protein-dependent activation of mast cell by peptides and basic secretagogues. Peptides 2002;23:1507-15.
93. Subramanian H, Gupta K, Guo Q, Price R, Ali H. Mas-related gene X2 (MrgX2) is a novel G protein-coupled receptor for the antimicrobial peptide LL-37 in human mast cells resistance to receptor phosphorylation, desensitization, and internalization. J Biol Chem 2011;286:44739-49.
94. Yu Y, Zhang Y, Zhang Y, Lai Y, Chen W, Xiao Z, et al. LL-37-induced human mast cell activation through G protein-coupled receptor MrgX2. Int Immunopharmacol 2017;49:6-12.
95. Tatemoto K, Nozaki Y, Tsuda R, Konno S, Tomura K, Furuno M, et al. Immunoglobulin E-independent activation of mast cell is mediated by Mrg receptors. Biochem Biophys Res Commun 2006;349:1322-8.
96. Kashem SW, Subramanian H, Collington SJ, Magotti P, Lambris JD, Ali H. G protein coupled receptor specificity for C3a and compound 48/80-induced degranulation in human mast cells: roles of Mas-related genes MrgX1 and MrgX2. Eur J Pharmacol 2011;668:299-304.
97. Varricchi G, Pecoraro A, Loffredo S, Poto R, Rivellese F, Genovese A, et al. Heterogeneity of human mast cells with respect to MRGPRX2 receptor expression and function. Front Cell Neurosci 2019;13:299.
98. Reddy VB, Graham TA, Azimi E, Lerner EA. A single amino acid in MRGPRX2 necessary for binding and activation by pruritogens. J Allergy Clin Immunol 2017;140:1726-8.
99. Alkanfari I, Gupta K, Jahan T, Ali H. Naturally occurring missense MRGPRX2 variants display loss of function phenotype for mast cell degranulation in response to substance P, hemokinin-1, human β-defensin-3, and icatibant. J Immunol 2018;201:343-9.
100. Zhang T, Che D, Liu R, Han S, Wang N, Zhan Y, et al. Typical antimicrobials induce mast cell degranulation and anaphylactoid reactions via MRGPRX2 and its murine homologue MRGPRB2. Eur J Immunol 2017;47:1949-58.
101. Pałgan K, Kuźmiński A, Janik A, Gotz-Żbikowska M, Bartuzi Z. Snake (*Vipera berus*) bite: the cause of severe anaphylactic shock and hepatocellular injury. Int J Immunopathol Pharmacol 2015;28:119-21.
102. Campbell EM, Charo IF, Kunkel SL, Strieter RM, Boring L, Gosling J, et al. Monocyte chemoattractant protein-1 mediates cockroach allergen-induced bronchial hyperreactivity in normal but not CCR2−/− mice: the role of mast cells. J Immunol 1999;163:2160-7.
103. Lukic A, Larssen P, Fauland A, Samuelsson B, Wheelock CE, Gabrielsson S, et al. GM-CSF– and M-CSF–primed macrophages present similar resolving but distinct inflammatory lipid mediator signatures. FASEB J 2017;31:4370-81.
104. Ohradanova-Repic A, Machacek C, Fischer MB, Stockinger H. Differentiation of human monocytes and derived subsets of macrophages and dendritic cells by the HLDA10 monoclonal antibody panel. Clin Transl Immunology 2016;5:e55.
105. Daigneault M, Preston JA, Marriott HM, Whyte MK, Dockrell DH. The identification of markers of macrophage differentiation in PMA-stimulated THP-1 cells and monocyte-derived macrophages. PLoS One 2010;5:e8668.
106. Zamani F, Shahneh FZ, Aghebati-Maleki L, Baradaran B. Induction of CD14 expression and differentiation to monocytes or mature macrophages in promyelocytic cell lines: new approach. Adv Pharmaceut Bull 2013;3:329.
107. Chen R-F, Wang L, Cheng J-T, Yang KD. Induction of IFNα or IL-12 depends on differentiation of THP-1 cells in dengue infections without and with antibody enhancement. BMC Infect Dis 2012;12:340.
108. Paulsen K, Tauber S, Dumrese C, Bradacs G, Simmet DM, Gölz N, et al. Regulation of ICAM-1 in cells of the monocyte/macrophage system in microgravity. BioMed Res Int 2015;2015:538786.
109. Ding J, Lin L, Hang W, Yan X. Beryllium uptake and related biological effects studied in THP-1 differentiated macrophages. Metallomics 2009;1:471-8.
110. Starr T, Bauler TJ, Malik-Kale P, Steele-Mortimer O. The phorbol 12-myristate-13-acetate differentiation protocol is critical to the interaction of THP-1 macrophages with *Salmonella typhimurium*. PLoS One 2018;13:e0193601.
111. Tjabringa GS, Ninaber DK, Drijfhout JW, Rabe KF, Hiemstra PS. Human cathelicidin LL-37 is a chemoattractant for eosinophils and neutrophils that acts via formyl-peptide receptors. Int Arch Allergy Immunol 2006;140:103-12.
112. Agier J, Efenberger M, Brzezińska-Błaszczyk E. Cathelicidin impact on inflammatory cells. Cent Eur J Immunol 2015;40:225.
113. Yang J, Zhang L, Yu C, Yang X-F, Wang H. Monocyte and macrophage differentiation: circulation inflammatory monocyte as biomarker for inflammatory diseases. Biomarker Res 2014;2:1.

114. Guilliams M, Ginhoux F, Jakubzick C, Naik SH, Onai N, Schraml BU, et al. Dendritic cells, monocytes and macrophages: a unified nomenclature based on ontogeny. Nat Rev Immunol 2014;14:571-8.
115. Bowman EP, Kuklin NA, Youngman KR, Lazarus NH, Kunkel EJ, Pan J, et al. The intestinal chemokine thymus-expressed chemokine (CCL25) attracts IgA antibody-secreting cells. J Exp Med 2002;195:269-75.
116. Vujicic M, Saksida T, Despotovic S, Bajic SS, Lalić I, Koprivica I, et al. The role of macrophage migration inhibitory factor in the function of intestinal barrier. Sci Rep 2018;8:1-12.
117. Ko IK, Kim B-G, Awadallah A, Mikulan J, Lin P, Letterio JJ, et al. Targeting improves MSC treatment of inflammatory bowel disease. Mol Ther 2010;18:1365-72.
118. Almeida CR, Caires HR, Vasconcelos DP, Barbosa MA. NAP-2 secreted by human NK cells can stimulate mesenchymal stem/stromal cell recruitment. Stem Cell Rep 2016;6:466-73.
119. Jiang J, Jin W, Peng Y, Liang X, Li S, Wei L, et al. The role of Cortistatin-14 in the gastrointestinal motility in mice. Pharmacol Rep 2018;70:355-63.
120. Gonzalez-Rey E, Varela N, Sheibanie AF, Chorny A, Ganea D, Delgado M. Cortistatin, an antiinflammatory peptide with therapeutic action in inflammatory bowel disease. Proc Natl Acad Sci 2006;103:4228-33.
121. Huynh E, Penney J, Caswell J, Li J. Protective effects of protegrin in dextran sodium sulfate-induced murine colitis. Front Pharmacol 2019;10:156.
122. Gupta K, Kotian A, Subramanian H, Daniell H, Ali H. Activation of human mast cells by retrocyclin and protegrin highlight their immunomodulatory and antimicrobial properties. Oncotarget 2015;6:28573.
123. Brinkman DJ, Ten Hove AS, Vervoordeldonk MJ, Luyer MD, de Jonge WJ. Neuroimmune interactions in the gut and their significance for intestinal immunity. Cells 2019;8:670.
124. Lai NY, Mills K, Chiu IM. Sensory neuron regulation of gastrointestinal inflammation and bacterial host defence. J Intern Med 2017;282:5-23.
125. Chompunud Na Ayudhya C, Roy S, Thapaliya M, Ali H. Roles of a mast cell–specific receptor MRGPRX2 in host defense and inflammation. J Den Res 2020;99:882-90.
126. Chávez-Galán L, Olleros ML, Vesin D, Garcia I. Much more than M1 and M2 macrophages, there are also CD169+ and TCR+ macrophages. Front Immunol 2015;6:263.
127. Ruytinx P, Proost P, Van Damme J, Struyf S. Chemokine-induced macrophage polarization in inflammatory conditions. Front Immunol 2018;9:1930.
128. Zhu Y, Zhang L, Lu Q, Gao Y, Cai Y, Sui A, et al. Identification of different macrophage subpopulations with distinct activities in a mouse model of oxygen-induced retinopathy. Int J Mol Med 2017;40:281-92.
129. Vianello E, Dozio E, Arnaboldi F, Marazzi M, Martinelli C, Lamont J, et al. Epicardial adipocyte hypertrophy: association with M1-polarization and toll-like receptor pathways in coronary artery disease patients. Nutr Metab Cardiovasc Dis 2016;26:246-53.